Comparative transcriptome analysis of PBMC from HIV patients pre- and post -antiretroviral therapy

Short title: Comparative transcriptome analysis of ART to HIV

Authors and Affiliations

Fang Zhao[1¶], Jingmin Ma[2,3¶] , Lihua Huang[2¶], Yong Deng[1], Liqiang Li[2] , Yang Zhou[1] , Jiandong Li[2] , Shaxi Li[1] , Hui Jiang[2], Huanming Yang[2,6], Shan Gao[7], Hui Wang[1,2,4,5]*, Yingxia Liu[1]*

[1] Shenzhen Third People's Hospital, Shenzhen, China

[2]Beijing Genome Institute, Shenzhen, China

[3]Department of Biology, University of Copenhagen, Copenhagen, Denmark

[4]Department of Zoology, University of Oxford, Oxford, UK

[5]NERC/Centre for Ecology & Hydrology Wallingford, Oxfordshire, UK

[6]James D. Watson Institute of Genome Science, Hangzhou, China

[7]CAS Key Laboratory of Biomedical & Diagnostic Technology, CAS/Suzhou Institute of Biomedical Engineering and Technology, Suzhou, China

Correspondence to *huiwang789@gmail.com* and *yingxialiu@hotmail.com

¶These authors contributed equally to this work.

Abstract

Infections of the human immunodeficiency virus (HIV) trigger host immune responses, but the virus can destroy the immune system and cause acquired immune deficiency syndrome (AIDS). Highly active antiretroviral therapy (HAART) can suppress viral replication and restore the impaired immune function. To understand HIV interactions with host immune cells during HAART, the transcriptomes of peripheral blood mononuclear cells (PBMC) from HIV patients and HIV negative volunteers before and two weeks after HAART initiation were analyzed using RNA sequencing (RNA-Seq) technology. Differentially expressed genes (DEGs) in response to HAART were firstly identified for each individual, then common features were extracted by comparing DEGs among individuals and finally HIV-related DEGs were obtained by comparing DEGs between the HIV patients and HIV negative volunteers. To demonstrate the power of this approach, minimum numbers of patients (one HIV alone; one HIV + tuberculosis, TB; one HIV+TB with immune reconstitution inflammatory syndrome during HAART) and two HIV negative volunteers were used. More than 15,000 gene transcripts were detected in each individual sample. Fourteen HAART up-regulated and eleven down-regulated DEGs were specifically identified in the HIV patients. Among them, nine up-regulated (*CXCL1, S100P, AQP9, BASP1, MMP9, SOD2, LIMK2, IL1R2* and *BCL2A1*) and nine down-regulated DEGs (*CD160, CD244, CX3CR1, IFIT1, IFI27, IFI44, IFI44L, MX1* and *SIGLEC1*) have already been reported as relevant to HIV infections in the literature, which demonstrates the credibility of the method. The newly identified HIV-related genes (up-regulated: *ACSL1, GPR84, GPR97, ADM, LRG1*; down-regulated: *RASSF1, PATL2*) were empirically validated using qRT-PCR. The Gene Set Enrichment Analysis (GSEA) was also used to determine pathways significantly affected by HAART. GSEA further confirmed the HAART relevance of five genes (*ADM*, *AQP9*, *BASP1*, *IL1R2* and *MMP9*). The newly identified HIV-related genes, *ADM* (which encodes Adrenomedullin), a peptide hormone in circulation control, may contribute to HIV-associated hypertensions, providing new insights into HIV pathology and

novel strategies for developing anti-HIV target. More importantly, we demonstrated that comparative transcriptome analysis is a very powerful tool to identify infection related DEGs using a very small number of samples. This approach could be easily applied to improve the understanding of pathogen-host interactions in many infections and anti-infection treatments.

Keywords

HIV, HAART, RNA-seq, PBMC, transcriptome

1.Introduction

Human immunodeficiency virus-1 (HIV-1) is a retrovirus that primarily infects components of the human immune system, such as CD4+ T cells, macrophages and dendritic cells [1]. HIV directly and indirectly destroys CD4+ T cells, which leads to severe immunodeficiency and increased susceptibility to opportunistic infections in most infected patients [2]. In addition, HIV also induces chronic immune activation, including cells involved in the innate immunity and acquired immunity, not only during the early phases of the infection but also throughout the chronic phase [3]. The state of chronic immune activation contributes to the loss of CD4+ T cells and changes in the immune responses, ultimately leading to disease progression [4]. Highly active antiretroviral therapy (HAART) can suppress viral replication, reduce the virus load in a patient's body and partially restore circulating CD4+ T cells to allow the immune system to combat HIV infections [5]. However, the side effects of this treatment may accumulate and problems including HIV-associated hypertension disorders[6] and cardiovascular disease[7] may emerge in certain patients during antiretroviral therapy (ART). Because an increasing number of patients suffer from drug toxicity, the emergence of drug resistant viruses and immune reconstitution inflammatory syndrome (IRIS) following the initiation of HAART represent new challenges in the battle against AIDS [8, 9].

Genome-wide gene expression profiling is an informative method used to reveal global changes of the

immune system in health and/or disease conditions. It has been particularly useful in identifying biomarkers, examining disease states and investigating immune responses [10]. Although a number of transcriptomic studies of HIV infection have been conducted, most were based on microarray technologies that focused on a limited number of genes [11-15]. Thus, these methods are limited in their capacity to detect novel gene products that interact with the virus infection. Recently, next-generation sequencing (NGS) technology has provided a new methodology to both identify and quantify the gene transcripts detected in transcriptome studies [16]. This method, termed RNA-Seq (RNA sequencing), provides highly accurate measurements of genome-wide gene expression via high-throughput NGS sequencing and generates high quality transcriptomic data. This approach yields a plethora of information, including transcript abundance, gene structure, alternative splicing, profiles of non-coding RNA species and genetic polymorphisms [17-19]. RNA-Seq has been applied in HIV-1 studies. For example, Stewart T. *et al.* used this technology to examine mRNA and MicroRNA changes in the transcriptome of CD4+ T cells infected with HIV in culture [20, 21]. Ming D. *et al.* sequenced RNA transcripts in the brain of HIV-1 transgenic rats to identify differentially expressed genes (DEGs) and enriched pathways affected by the HIV transgene in different areas of the brain [22]. However, few studies have examined the utility of comparative transcriptomic analysis based on RNA-seq to investigate HIV-host interactions in samples from HIV patients, especially the transcriptional changes of host genes after HAART.

Many genome-wide expression studies of HIV infection are based on an analysis of total peripheral blood mononuclear cells (PBMCs) [14, 23-25], which consist of over a dozen cell subsets, including T cells, B cells, NK cells and monocytes. Although the specific gene expression signals of particular cell subsets will be diluted by those from the other cells and thus reduce the specificity of this approach [12, 15, 21], PBMC is a good starting material to obtain generic information against HIV infection.

In this study, we investigated changes in the transcriptomes of PBMCs from HIV positive patients and

HIV negative volunteers before and two weeks after HAART using RNA-Seq technology. To demonstrate the power of this approach, small cohorts (three HIV patients and two HIV negative volunteers) were used. We firstly identified the differentially expressed genes (DEGs) for the time course of each individual. The shared DEGs among individuals were then used to enable comparisons between the HIV patients and HIV negative volunteers. All DEGs were validated empirically by qRT-PCR. The Gene Set Enrichment Analysis (GSEA) was also used to identify pathways that were significantly affected by HAART. These analyses revealed new gene expression patterns of PBMCs and provided new insights into the pathogenesis of HIV-induced immune suppression and HIV-TB associated gene expression changes during HAART. Such an individual comparative transcriptome approach did not require large sample cohort thus could be valuable for future practice of precision medicine.

2. Materials and Methods

2.1.Ethics Statement

The study protocol was approved by the Institutional Review Board of the Shenzhen Third People's Hospital. Written informed consent was obtained from all participants.

2.2.Treatment-naïve HIV infected and HIV negative individuals

Three HIV-infected individuals and two HIV-negative volunteers were recruited at the Shenzhen Third People's Hospital from April 2013 to September 2013 (Table 1). Two healthy persons who putatively exposed to HIV and proactively requested HAART were proved to be free of HIV infection by ELISA and HIV RNA testing one month later. All participants were screened for HIV antigens and antibodies via standard ELISA analyses, and these findings were further confirmed by Western Blotting. CD4 counts were

obtained by flow cytometry, and the viral loads were measured by qRT-PCR. Two of the three HIV serum-positive patients were also diagnosed as being positive for *B. tuberculosis*, as assessed by microbiology tests (sputum acid fast bacilli stain or cultures on Lowenstein–Jensen media). All clinical tests mentioned above were performed by the hospital clinical laboratory, which has a certified license issued by the National AIDS Reference Laboratory at China CDC.

Treatment for the diagnosed HIV-TB patients consisted of standard fixed-dose chemotherapy for two weeks with isoniazid (H), ethambutol (E), rifampicin (R) and pyrazinamide (Z), followed by a combination of highly active antiretroviral therapy (HAART) and anti-TB treatment (HERZ) [26]. The HAART regimen consisted of zidovudine plus lamivudine with efavirenz, which is the recommended anti-HIV treatment regimen in China [27].

2.3. Sample collection, PBMC isolation, RNA extraction and RNA-Seq sequencing

In total, 10 blood samples (5 mL per sample) from five participants were collected at two different time points: immediately before and two-weeks after the start of HAART. The total RNA was extracted from each PBMC sample using the Qiagen RNeasy kit (QIAGEN). The RNA concentration and quality were measured using an Agilent 2100 Bioanalyzer (Agilent), and these analyses showed that all RNA samples had an RNA integrity number (RIN) of >7.5 and a 28S:18S rRNA ratio of >1.8. Beads containing oligo (dT) were used to isolate poly(A)-tailed mRNA from the total RNAs. The Purified mRNAs were used to construct RNA-Seq libraries, which were sequenced on an Illumina HiSeq 2000 sequencing platform (using TruSeqV3 sequencing reagents) at the BGI-shenzhen (Expected library size: 200bp; Read length: 90 nt; and Sequencing strategy: paired-end sequencing) as described in previous article[28].

2.4.Mapping reads to the human genome and transcriptome database

The reference sequences used in this study were the human genome and transcriptome sequences downloaded from the UCSC website (http://genome.ucsc.edu/index.html, version hg19). After the removal of low quality reads, clean reads were aligned to the reference genome or transcriptome using SOAP2 [29]. No more than five mismatches were allowed in the alignment of each read.

2.5. Normalization of gene and long non-coding RNA expression levels

Reads that could be uniquely mapped to a reference gene were used to calculate the expression level. The gene expression level was measured based on the number of uniquely mapped reads per kilo-base of exon region per million mapped reads (RPKM). The formula is defined below:

$$\mathrm{RPKM} = \frac{10^6 \mathrm{C}}{\mathrm{NL} \div 10^3} = \frac{\mathrm{C} * 10^9}{\mathrm{N} * \mathrm{L}}$$

in which C is the number of reads uniquely mapped to the given gene; N is the number of reads uniquely mapped to all genes; L is the total length of exons from the given gene. For genes with more than one alternative transcript, the longest transcript was used to calculate the RPKM. The RPKM method eliminates the influence of different gene lengths and sequencing discrepancies on the gene expression calculation. Therefore, the RPKM value can be directly used to compare the differences in gene expression among samples. Based on RPKM, a global expression plot was produced to compare the expression profiles before and after HAART for each HIV-patient and HIV-negative volunteer.

2.6. Principal Component Analysis (PCA)

The R software (http://stat.ethz.ch/R-manual/R-patched/library/stats/html/prcomp.html), which is based on the RPKM value of each gene of the samples, was used to group and perform the PCA analysis of the

expression level with a cumulative proportion of principal component 1 (48.16%) and principal component 2 (26.49%) of 0.75. A scatter figure was then drawn based on principal component 1 and principal component 2.

2.7. Differentially expressed gene (DEG) analysis and Gene Ontology (GO) Enrichment

Using the NOISeq program [30], we identified DEGs by comparing the expression level of the post-HAART sample to that of the pre-HAART sample from the same individual according to the following criteria and the DEG must meet condition: Probability>= 0.8 and fold change>=2. We then used the DAVID tools [31] to annotate and enrich the significant DEGs to certain Gene Ontology terms. The threshold for the GO enrichment analysis was an ease-score <=0.05 and p value < 0.05.

2.8. Gene Set Enrichment Analysis

Gene Set Enrichment Analysis (GSEA) is a computational method for association studies by examining whether the expression profile of a certain gene set have a significant tendency between two concerned biological states[32] (in this study, before and after HAART). Genes were ranked in descending order based on RPKM using the weighted log2 ratio of Classes metric. Nominal p values were calculated based on permutation tests using gene set permutation with 1000 permutations without balancing. The hallmark gene sets derived from the Molecular Signature Database (MSigDB) were selected for GSEA. Normalized enrichment scores were calculated as previously described using the GSEA software (version 2.2.0) and gene sets were ranked accordingly. False discovery rate (FDR) <0.05 was considered to be statistically significant.

2.9. Quantitative real time PCR validations of differentially expressed genes

To confirm the results obtained from the RNA-Seq analysis, we conducted quantitative real-time RT-PCR (qRT-PCR), the commonly used quantification method for studying gene expression. In brief, the total RNA from each sample was used for reverse transcription [33] with random primers N6 and the PrimeScript™kit (PrimeScript™ One Step RT-PCR Kit Ver.2, TaKaRa) for cDNA synthesis. The cDNA was then subjected to qPCR in a 96-well format in triplicate reactions [34] with defined primers (Supplementary Table S1) and SYBR® Green (One Step SYBR PrimeScript RT-PCR Kit, TaKaRa). The qPCR reactions were performed using StepOnePlus™ Real-Time PCR Systems (Applied Biosystem). The expression levels of all genes were normalized to the expression level of the housekeeping gene *β-actin* and then analyzed with the comparative $C_T(\Delta\Delta C_T)$ method [35].

3. Results

3.1. Clinical characteristics of enrolled subjects

Table 1: Clinical profiles of the HIV patients and healthy controls used in this study

				before ART		**2w after ART**		
	Infection situation	**Age**	**Gender**	**Viral load (copies/mL)**	**CD4 (cells/μl)**	**Viral load (copies/mL)**	**CD4 (cells/μl)**	**IRIS**
P1	HIV&TB	31	Male	6.08E+07	100	2.89E+02	416	Yes
P2	HIV&TB	45	Male	2.82E+04	213	3.54E+02	235	No
P3	HIV	32	Male	1.08E+05	121	8.76E+03	168	No
H1	Health control	29	Male	NA	756	NA	730	No
H2	Health control	27	Male	NA	623	NA	660	No

ART: Antiretroviral therapy; TB: tuberculosis; NA: not available; IRIS: Immune Reconstitution Inflammatory Syndrome;

Three HIV-infected patients (P1, P2 and P3) and two healthy controls (H1 and H2) were enrolled in this study. Table 1 shows the clinical records pre- and post-HAART. As expected, the CD4-cell counts did not significantly change in the two healthy controls (H1 and H2). In all HIV-patients (P1-3), the CD4-cell counts increased after HAART, coupled with a dramatic decrease in the HIV load. This finding demonstrated that the HAART effectively controlled HIV replication and allowed the host immune system to recover. Compared to that of P1 patient, the CD4-cell counts of P2 and P3 patients were mildly increased (less than two-fold) even though their virus load reduced by approximately two orders of magnitude (Table 1). P1 had a high virus load of 6.08E+07 copies/mL before treatment. After two weeks of HAART, the virus load was reduced to 2.89E+02 copies/ml. Moreover, P1 showed the best restoration of CD4-cell count among the three patients, with more than three-fold increase in CD4-cell count (from 100 cells/μl at pre-treatment to 416 cells/μl at post-treatment (Table 1). However, this patient developed TB-IRIS during HAART (data not shown), which is a reflection of the high risk for the HIV patients that undergo HAART to develop IRIS

3.2. Profiling of the PBMC transcriptomes by Overview of the RNA-Seq

RNA-seq was applied to characterize the transcriptome profile of PBMCs from subjects. Each raw dataset of the samples contained between 46 and 60 million reads, with an average of approximately 58 million raw reads (5.2 GB of data) per sample. More than 97% bases had a quality score of ≥ Q20. Approximately $39\sim52 \times 10^6$ reads (78%-81% of the total raw reads) were aligned to the human genome sequence (Build hg19) in each of the samples (Table S1), giving an average of 50 million human reads per sample for further analyses.

The reads that had been uniquely aligned to the transcript sequencing (by RefSeq) were subsequently analyzed using the BGI in-house package suites for transcripts abundance normalization and evaluation [28]. More than 15,000 transcripts were detected in all individuals, while the average of expressed genes was 17,135. All transcripts of each sample were filtered with a coverage cutoff value of RPKM > 0.7. Using RPKM of the qualified the genes, a global expression plot was produced for each individual (Supplementary Fig. S1).

Principal Component Analysis (PCA) was performed on those datasets to compare the similarity and variability of gene expression profiles among subjects. Component 1 contribute 48.16% and component 2 contribute 26.49% of the whole transcriptome. All the samples were detected about 17,000 genes for PCA analysis. The PCA results (Fig. 1) indicated that patient P1, who developed a TB-IRIS, had transcriptome signature distinct from those of the other patients at both pre- and post-HAART, whereas the transcriptomes of P2, P3, H1 and H2 clustered together and displayed similar gene expression profiles (Fig. 1). Given that P1 developed TB-IRIS, it is tempting to speculate that the complication of TB-IRIS was accountable for the reprogramming of the host's whole transcriptome Furthermore, the striking alteration in the transcriptome of P1 at pre- vs post-treatment (Fig 1) was likely to be a real demonstration of the effectiveness of HAART, in light of the dramatic decline of viral load and the considerable recovery of CD4-cells (Table 1). Though further investigations are needed to pinpoint the underlying causes of the aberrant transcriptomes in P1, the singular transcriptional profiles of P1 were consistent with the unique clinical features of this patient.

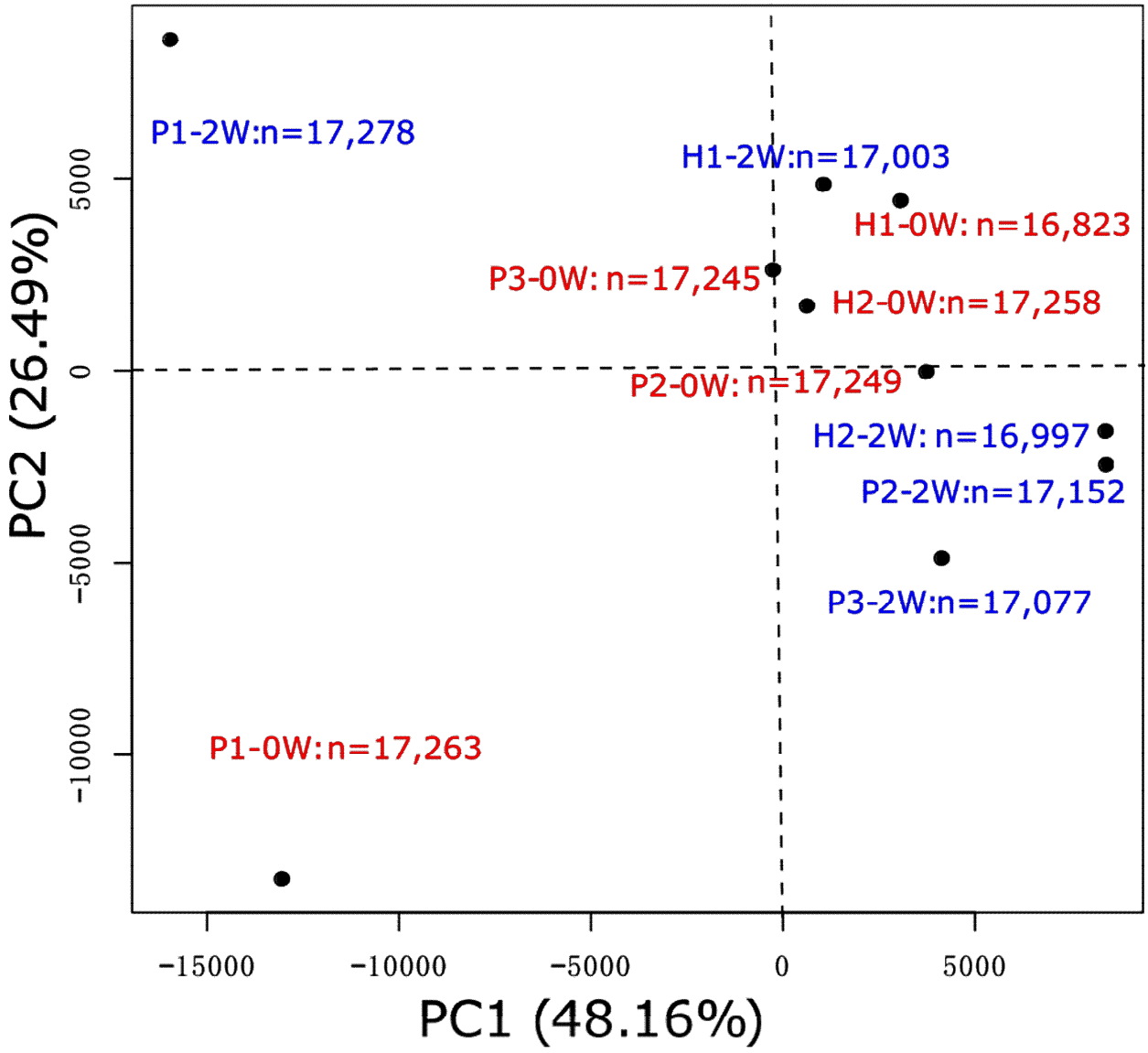

Figure 1. Principal Component Analysis (PCA) of gene expressions in all samples. 0W marked as red denotes before HAART, 2W marked as blue denotes two weeks after HAART started. The labelled number shows the gene numbers used for each sample.

3.3. Identification of HAART-induced differentially expressed genes (DEGs)

Even though the total number of genes detected in each subject exceeded 15,000, the numbers of DEGs in each individual varied greatly, ranging from >2000 (e.g.P3) to <50 (e.g.H1) (Fig. 2A, Supplementary Fig. S1 and Supplementary Table S3 and S4). H1 control had the minimal DEGs in response to HAART (number 42), while P3 had the most DEGs induced by HAART (number 2,083) (Fig 2A). More DEGs were

up-regulated than down-regulated by HAART in P1 and H1, while the opposite was observed for DEGs in P2, P3 and H2 (Fig. 2A, Supplementary Fig. S1 and Supplementary Table S3 and S4). These results indicated significant inter-individual variations in the DEG profiles in response to HAART (Fig. 2B).

When all DEGs were compared among these subjects, there was no DEG shared by all subjects, including the HIV-patients and controls. 25 DEGs (including 11 downregulated DEGs and 14 upregulated DEGs) were shared exclusively by three HIV-patients but not observed in controls (see below for details, Supplementary Table S3 and S4, Fig. 3A and Fig 3B). Only one DEG (a downregulated DEG) was shared by two controls only but not detected in HIV patients (Fig 3A and Fig 3B). In addition, three DEGs (including 1 downregulated DEG and 2 upregulated DEGs) were shared exclusively by HIV-TB patients (P1 and P2, Fig 3A and Fig 3B). Altogether, there were a total of 29 DEGs which were shared by at least two subjects. The lack of overlapping between the HAART-induced DEGs of HIV-patients with those of controls was indicative of the specific effects of HAART against HIV infection. The upregulated DEGs and downregulated DEGs were described in more detail respectively in the following two sections.

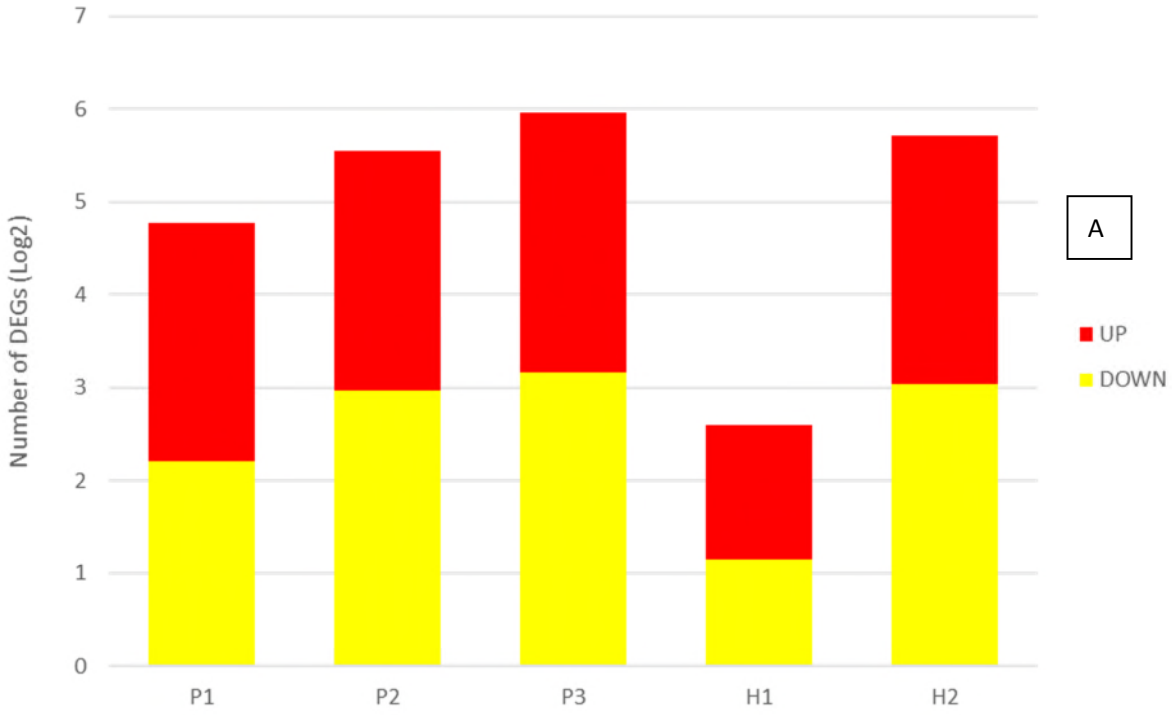

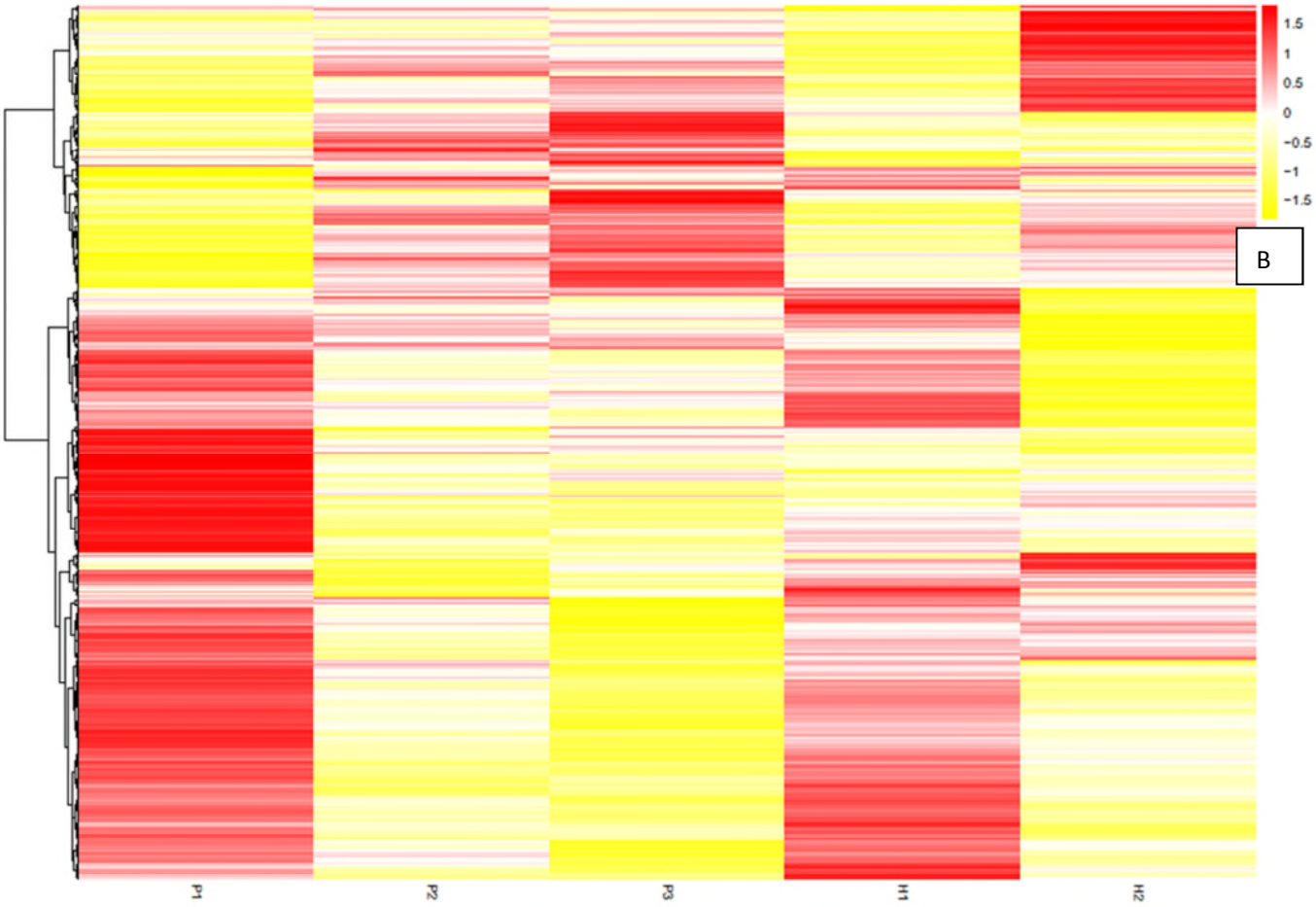

Figure 2. Analysis of differentially expressed genes (DEGs) at pre- and post- HAART. A: The number of DEGs for each individual. Red color labels the up-regulation genes and Yellow color labels down-regulation genes after HAART. B: DEGs rpkm value heatmap in each individual. Each line represents a DEG at least in one sample. Red color labels HAART up-regulated genes and yellow color labels HAART down-regulated genes.

3.4. HAART Down-Regulated Genes

All intersections of the genes down-regulated by HAART among the five individuals are displayed in Fig. 3A. The statistical threshold was set at a probability ≥ 0.8 and a fold change of ≥ 2 (NOISeq program [30]). As mentioned above, none of the down-regulated DEGs were shared by all individuals, as indicated by the zero DEG in the intersection of all DEG sets (Fig 3A). The intersections of healthy controls (H1 and H2)-specific, HIV patients(P1-3)-specific and HIV-TB patients (P1 and P2)-specific DEGs were selected for

further analyses. The expression changes (measured by RPKM values, Supplementary Table S4) of the selected DEGs were illustrated in a heat map for all individuals (Fig. 3B). A single DEG (*RNU2-1*) was shared by the healthy controls (H1 and H2) but not observed in the HIV patients. Apart from this *RNU2-1* gene, the DEG analysis supports that HAART exerts limited side effects on the transcriptome profiles of healthy individuals.

Eleven genes that were down-regulated by HAART were shared by all three HIV-patients(P1-P3) but not by normal controls (Fig. 3A). Among them, nine had already been reported for their relevance in HIV infections (Supplementary Table S2). The two newly determined genes that were specifically down-regulated in HIV-patients were *PATL2*, which encodes the protein associated with topoisomerase II homolog 2 and participates in RNA and protein binding, and *RASSF1*, which encodes the Ras association (RalGDS/AF-6) domain family member 1 and participates in tumor suppression and the induction of cell cycle arrest (Supplementary Table S2). A single DEG (*CDKN1C* encoding the Cyclin-dependent kinase inhibitor 1C) was shared by the two HIV-TB patients (Fig. 3A, P1 and P2), whose expression was not significantly changed in P3 and H1-2 (Fig. 3B), The alteration in CDKN1C expression might be specifically related to TB infection in HIV patients. A heat map cluster analysis (Fig. 3B) separated the two healthy controls (H1 and H2) from the three HIV-patients (P1-3) based on these 13 DEGs (including *RNU2-1* and *CDKN1C*). Among the HIV-patients, P2 and P3 were clustered together (Fig. 3B) and showed the distinct characteristics of the P1 transcriptome, which was also detected in Fig. 1. Two clusters, which were mainly the result of the DEG values, formed at the Y-axis of Fig. 3B. We have surveyed the gene in 2 cluster and find no significant enrichment in GO term of any cluster. So it may be just the difference in the range of down-regulation.

The down regulation of gene expression after HAART may due to normalization of expression that resulted from up-regulation after HIV infection. This can also be confirmed by the compare H1, H2 (control group)

vs P1, P2, P3 (patient group) before HARRT. We find 175 DEGs (Table S7) in totally which 129 (73.7%) of that was higher in patient group. Furthermore, 54.5% (6/11) of we detected down-regulated genes were higher in patient group than control group before HARRT while only 7.1% (1/14) of we detected up-regulated genes were lower in patient group.

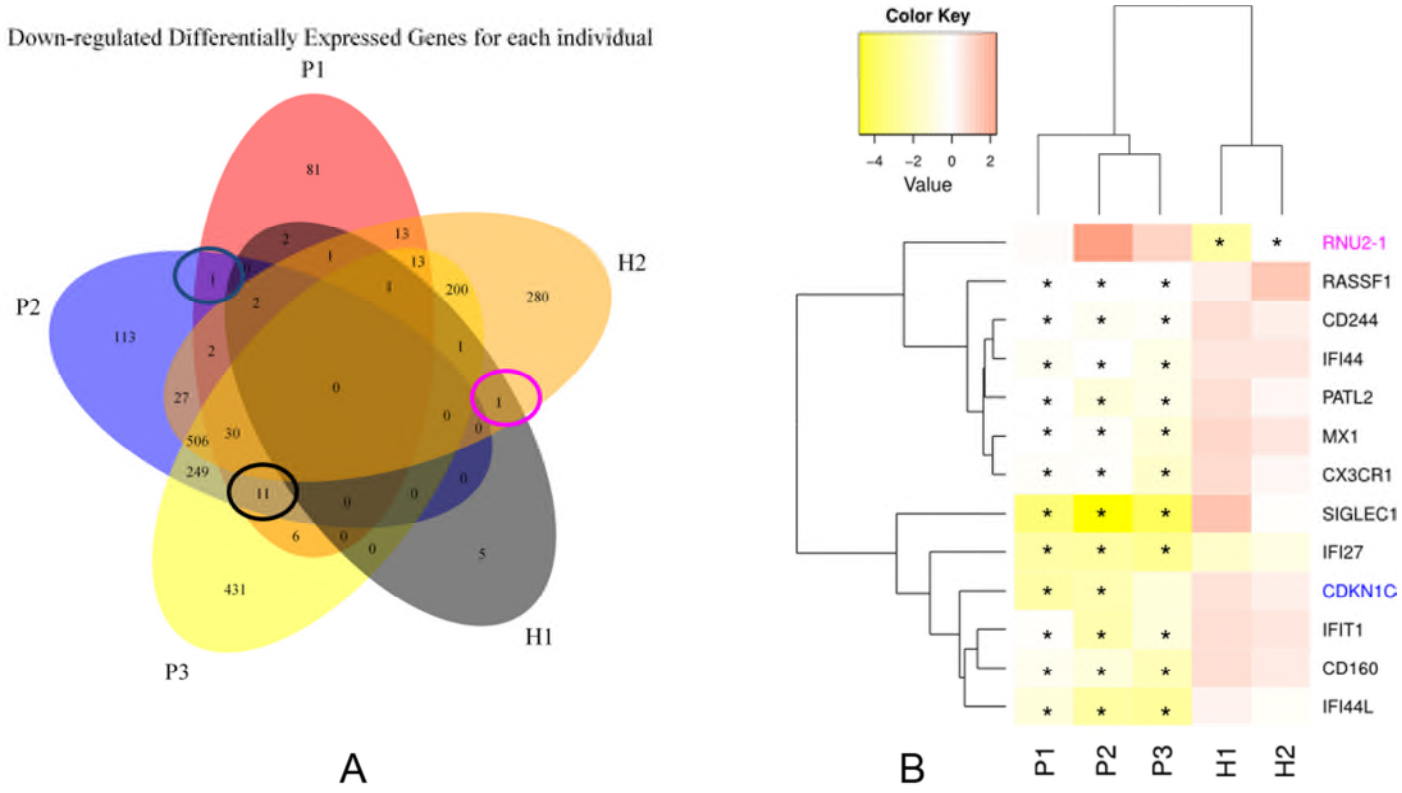

Figure 3. HAART down-regulated genes. Panel A: Down-regulated DEGs of each individual. Panel B: Heat cluster map of HAART down-regulated DEGs in Healthy control (H1 & H2, pink colour word labelling), HIV-patient (P1-3, black colour word labelling) and HIV-TB patient (P1 & P2, blue colour word labelling). Each DEG value was calculated using RPKM and represented by the formula of [log2(RPKM-after/RPKM-before HAART) -1], i.e., zero represents a two folds down-regulation. Star signs indicate where the gene expressions were statistically significantly changed.

3.5. HAART Up-Regulated Genes

As similarly to the down-regulated genes, none of the DEGs up-regulated by HAART were shared

among all five subjects (Fig. 4A), and none were shared by the two healthy controls (H1 and H2). The intersections were selected for the HIV patients (P1-3) and HIV-TB patients (P1 and P2). Fourteen of the genes up-regulated by HAART were shared by the three HIV patients (P1-3) but not the healthy controls (H1 and H2) (Fig. 4A and Supplementary Fig. S1). The relevance of nine of these genes in HIV has already been reported (Supplementary Table S3). We identified five novel genes whose expressions were elevated by HAART and might be thus suppressed by HIV replication (Fig. 4B, Supplementary Table S3): *ACSL1*, which encodes the acyl-CoA synthetase long-chain family member 1; *ADM*, which encodes the adrenomedullin; *GPR84*, which encodes the G protein-coupled receptor 84; *GPR97*, which encodes the G protein-coupled receptor 97; and LRG1, which encodes the leucine-rich alpha-2-glycoprotein 1. Based on the expression changes of these 14 HAART-up-regulated genes, P2 and P3 were again clustered together and differed from P1 (Fig. 4B), as also demonstrated in Fig. 1 and Fig. 3B. Two more genes were identified only in the HIV-TB patients: *SFXN1*, which encodes sideroflexin-1, and *SOCS3*, which encodes the suppressor of cytokine signaling 3 (Fig. 4B, Supplementary Table S3). The relevance of these two genes in HIV infection has already been reported in the literature (Supplementary Table S3). Again, the negative result in P3 either suggested that the DEG stringency were set excessively high or these genes might be affected by the TB co-infection.

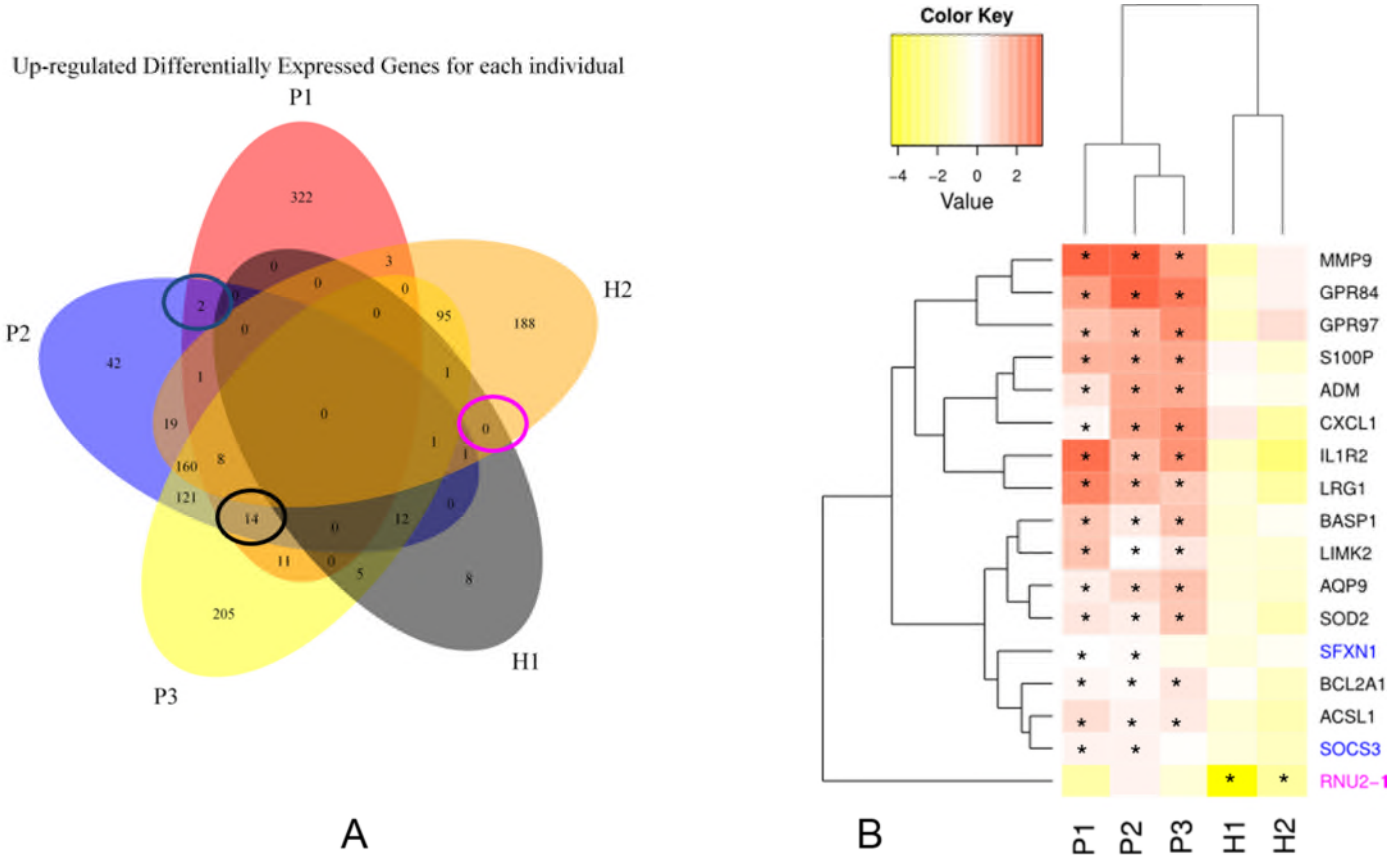

Figure 4. HAART up-regulated genes. Panel A: Up-regulated DEGs for each individual. Panel B: Heat cluster map of HAART down-regulated DEGs in Healthy control (H1 & H2, pink colour word labelling), HIV-patient (P1-3, black colour word labelling) and HIV-TB patient (P1 & P2, blue colour word labelling). Each DEG value was calculated using RPKM and represented by the formula of [log2(RPKM-before/RPKM-after HAART) -1], i.e., zero represents a two fold up-regulation. Star signs indicate where the gene expressions were statistically significantly changed.

3.6. Validation of the HAART induced DEGs by qRT-PCR

All of the 29 DEGs shown in Fig. 3 and 4 were experimentally validated using qRT-PCR. The qRT-PCR results confirmed our RNA-Seq observations with a 100% precision for the HAART up- and down-regulated genes in the HIV patients (Supplementary Table S4). Fig. 5 shows the qRT-PCR results in the heat map format. The QRT-PCR result conformed to the RNA-Seq result, which showed that the DEG

profiles of the healthy control (H1 and H2) differed from those of HIV patients (P1-3), as shown in the cluster tree at the X-axis in Fig. 5. Among the HIV patients, P2 and P3 were again clustered together, illustrating the isolation of P1. At the Y-axis (Fig. 5A-B), the qRT-PCR determined that the up- and down-regulated genes formed two main clusters, as detected by RNA-Seq analysis. None of the genes changed value was significant difference between qRT-PCR and RNA-seq (wilcoxon rank sum test, $p>0.05$).

The morphology of the clustering tree also showed similarities, e.g. *MX1*, *CX3CR1*, *PATL2*, *CD244* and *RASSF1* were clustered together, while *CD160*, *IFI27* and *SIGLEC1* were clustered in both the RNA-Seq and qRT-PCR heat maps (Figs. 3 and 5). In the HAART up-regulated gene section (Figs. 3 and 5), *ADM*, *CXCL1*, *S100P*, *MMP9*, *GPR84* and *LRG1* belonged to a cluster branch, whereas *ACSL1*, *LIMK2* and *BASP1* clustered in another branch. The DEG clustering relationships may not indicate functional connections, but they provide novel information on parallel gene expression changes in response to HAART. Most importantly, the consistency of the RNA-Seq and qRT-PCR results indicated that the comparative transcriptome approach we used can reliably identify HAART-induced DEGs.

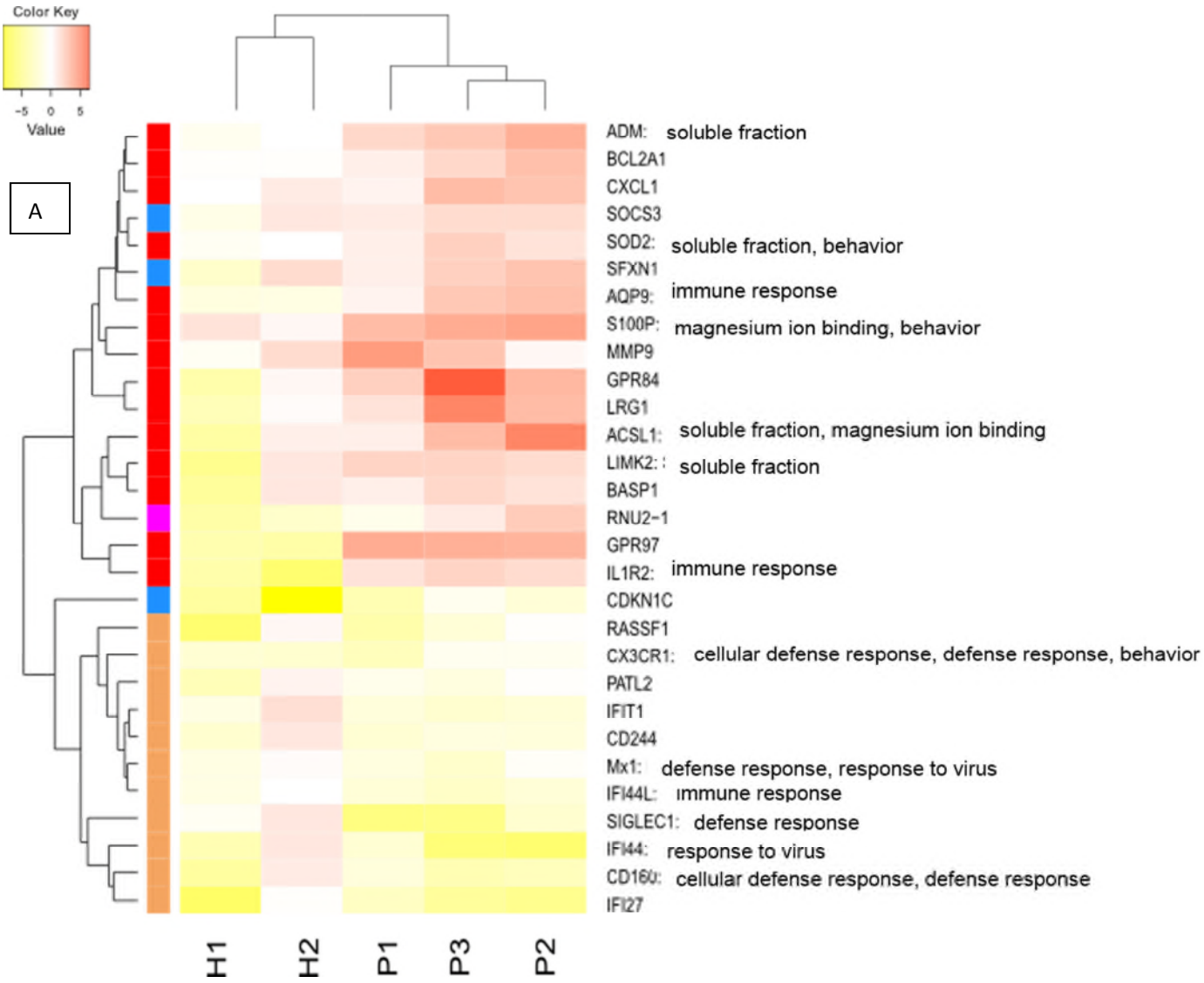
Color Key
-5 0 5
Value
A
ADM: soluble fraction
BCL2A1
CXCL1
SOCS3
SOD2: soluble fraction, behavior
SFXN1
AQP9: immune response
S100P: magnesium ion binding, behavior
MMP9
GPR84
LRG1
ACSL1: soluble fraction, magnesium ion binding
LIMK2: soluble fraction
BASP1
RNU2-1
GPR97
IL1R2: immune response
CDKN1C
RASSF1
CX3CR1: cellular defense response, defense response, behavior
PATL2
IFIT1
CD244
Mx1: defense response, response to virus
IFI44L: immune response
SIGLEC1: defense response
IFI44: response to virus
CD160: cellular defense response, defense response
IFI27
H1
H2
P1
P3
P2

359

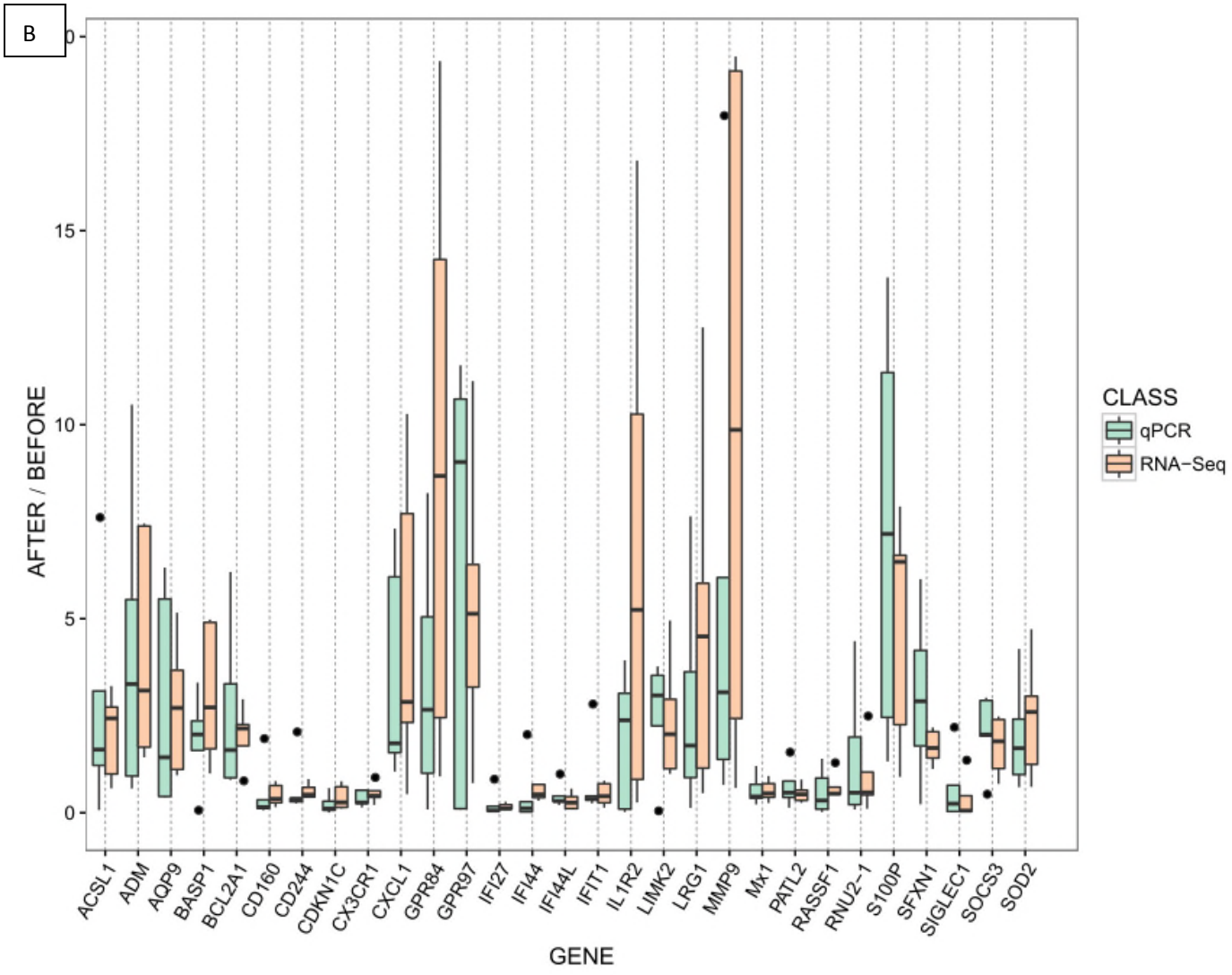

Figure 5. Quantitative real time PCR validations of differentially expressed genes. A: the cluster of the qPCR value calculated from after/before HAART. Yellow colour labelled heat map squares indicated HAART down-regulation and red colour labelling indicated HAART up-regulation. The colour coded column next to the cluster tree at Y-axis summarized the RNA-Seq results for HAART down-regulated (Brown) and up-regulated (Red) genes specific for the HIV patients (P1-3), HIV-TB patients (P1&2, Blue) and healthy controls (H1&2, Purple). **B**: Boxplot of each gene for the RNA-seq value and qPCR value calculated from after/before HAART.

3.7. Gene ontology (GO) analysis of HAART-induced DEGs in HIV patients

Next we assessed which cellular processes, biological functions or subcellular fractions were influenced by HAART in

HIV-infected individuals. First we used the perl package of GO-TermFinder-0.86 to draw the GO term enrichment figure (Fig. 6) for the whole set of 28 HIV infection relevant genes determined by RNA-seq (Figs. 3 and 4) and validated by qRT-PCR (Fig. 5). The 28 HIV-relevant genes were enriched in 39 GO terms at three levels (Biological process, cellular component and molecular function, Supplementary Table S5). The GO term biological adhesion was down-regulated by HAART (Fig. 6), demonstrating that the reduction of viral loads (Table 1) reduced the expressions of adhesion genes. Conversely, the genes in the GO terms of pigmentation, growth, reproduction, reproductive process, establishment of localization, localization, extracellular region part, extracellular region, transporter activity and antioxidant activity were all up-regulated, which shows that HIV activities suppressed the functions of these genes. The gene expressions in the other GO terms were not uniformly up-regulated or down-regulated, depending on the effect of the gene on the activity in the GO term (positive or negative effect).

All of the newly determined HIV infection-related genes (i.e. *PATL2* and *RASSF1* for HAART down-regulation; *ACSL1, ADM, GPR83, GPR97* and *LRG1* for HAART up-regulation; Supplementary Tables S2 & S3) were included in the GO terms of cellular process, cell and cell part (Fig. 6). *ADM* was involved in 21 of the 39 detected GO terms, suggesting that its expression might be up-regulated by HAART (thus down-regulated by HIV) in multiple pathways. Similarly, *RASSF1* and *PATL2* were included in 12 and 11 GO terms, respectively (Fig. 6), suggesting that the observed down-regulations by HAART might be due to more than a single functional change. Overall, Fig. 6 clearly shows that HAART which reduced the virus load in HIV patients induced many functional changes in PBMC(Table 1). Most importantly, the comparative transcriptome approach successfully detected these HIV-affected genes using a very small sample size, despite of the tremendous inter-individual variations (Fig. 1 and Supplementary Fig. S1). Then we restricted the input for GO analysis to 25 DEGs shared by all HIV patients in an attempt to obtain gene function information that is more specific to HIV infection. Generally, GO analysis revealed that

HAART regulated the expression of genes enriched in seven GO terms: soluble fraction, magnesium ion binding, immune response, behavior, defense response, cellular defense response, and response to virus. With respect to the HAART down-regulated DEGs in HIV patients, they fell into four GO terms, including soluble fraction, magnesium ion binding, immune response and behavior (Fig. 6, Supplementary Table S6). With regard to the HAART upregulated DEGs in HIV patients, they were enriched in the GO terms of immune response, behavior, defense response, cellular defense response, and response to virus (Fig 6, Supplementary Table S6). It is notable that genes involved in three cellular processes including defense response, cellular defense response, and response to virus were all upregulated by HAART in HIV patients (Fig 6, Supplementary Table S6), suggesting that without HAART, HIV would otherwise suppress the processes of cell defense and stress resistance in patients. In addition, immune response was revealed to be regulated by HAART in patients (Fig 6), which was quite expected. Taken together, these identified GO terms are consistent with the current knowledge on HIV-host interaction, which confirms that even on a small number of subjects, the RNA-seq based comparative transcriptome approach proves a powerful and sensitive tool to yield true biological insights.

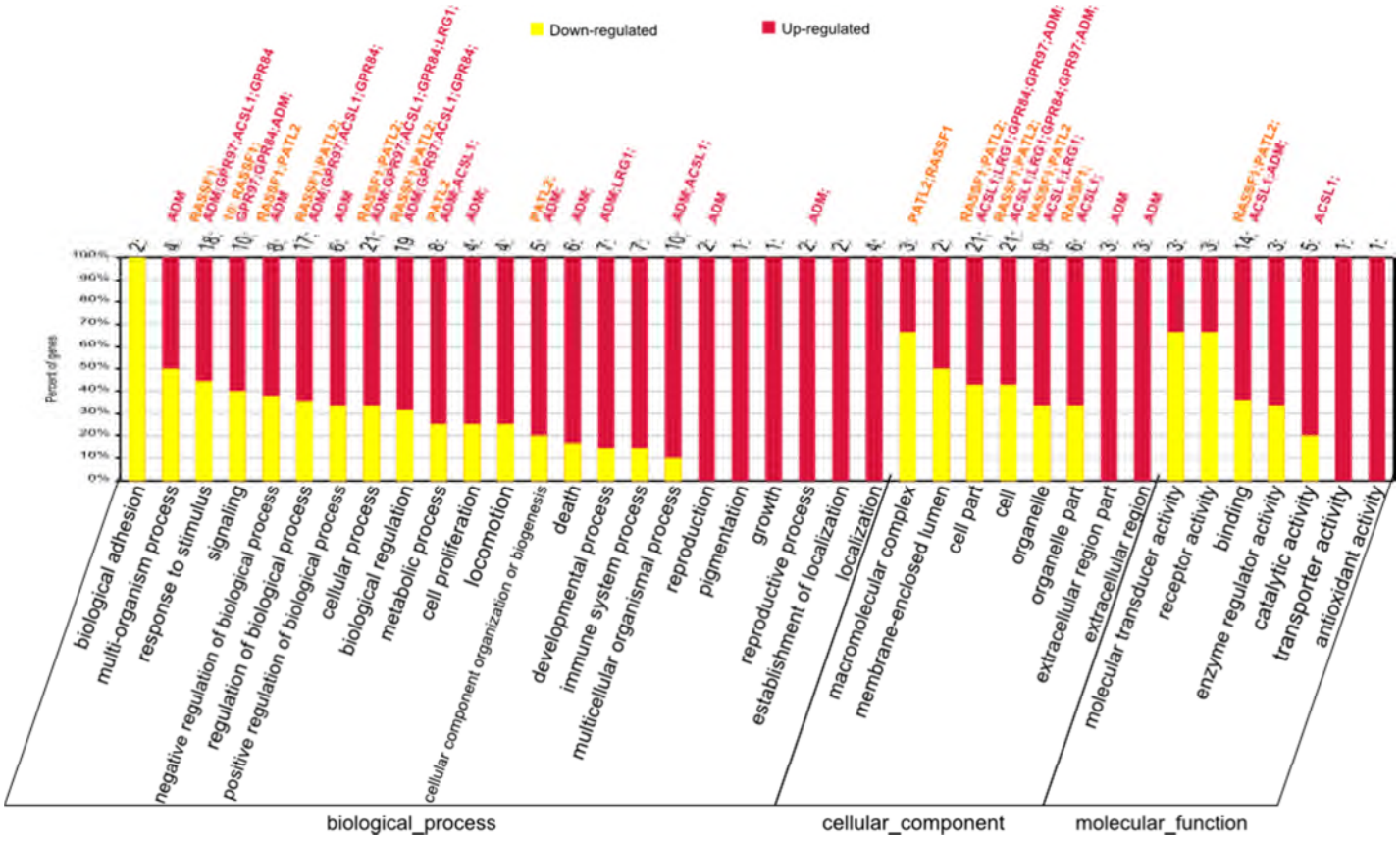

Figure 6. The enriched GO term of selected 28 differentially expressed genes. Red bars indicate the up-regulated genes, while yellow bars indicate the down-regulated genes. The X-axis indicates the enriched GO term, classified into 3 levels: biological process, cellular component and molecular function. The Y-axis shows the percentage of up- or down-regulated DEGs in certain GO term, the number above bars indicate the amount of 28 DEGs enriched into certain GO term with the names of the newly determined genes associated with HIV infection.

Gene Set Enrichment Analysis (GSEA)

To get a more comprehensive and biologically meaningful overview of HAART-regulated cellular processes, we conducted GSEA on the RNA seq data. Different to the DEG analysis, GSEA analysis the performance of a gene set (pathway) between the two samples. It also calculated the statistics using all biological replicates in a treatment, i.e., HIV patients and HIV negative volunteers in this study. Among the 50 pre-defined gene sets provided by the MSigDB, 14 pathways were upregulated specifically to the HIV

patients by HAART (Fig. 7). Seven pathways were upregulated in both HIV patients and the HIV negative volunteers in whom two more pathways were also upregulated by HAART (Fig. 7). In comparison, five HAART upregulated DEGs (*ADM*, *AQP9*, *BASP1*, *IL1R2* and *MMP9*, Fig. 4) were specific for the HIV patients (not being members of the gene sets identified for the HIV negative volunteers) (Supplementary Fig.S2). Among them, *ADM* was a new HIV related gene identified in this study (Fig.6). It encodes adrenomedullin, a peptide hormone which is involved in inflammatory response and hypoxia (Supplementary Fig.S2). The inflammatory response pathway also involves AQP9 (aquaporin 9) which has been reported for involvements of HIV-associated dementia [36]. The hypoxia gene set also contains *MMP9* encodes the matrix metallopeptidase 9 which activities are associated with cardiovascular diseases in HIV patients [37].

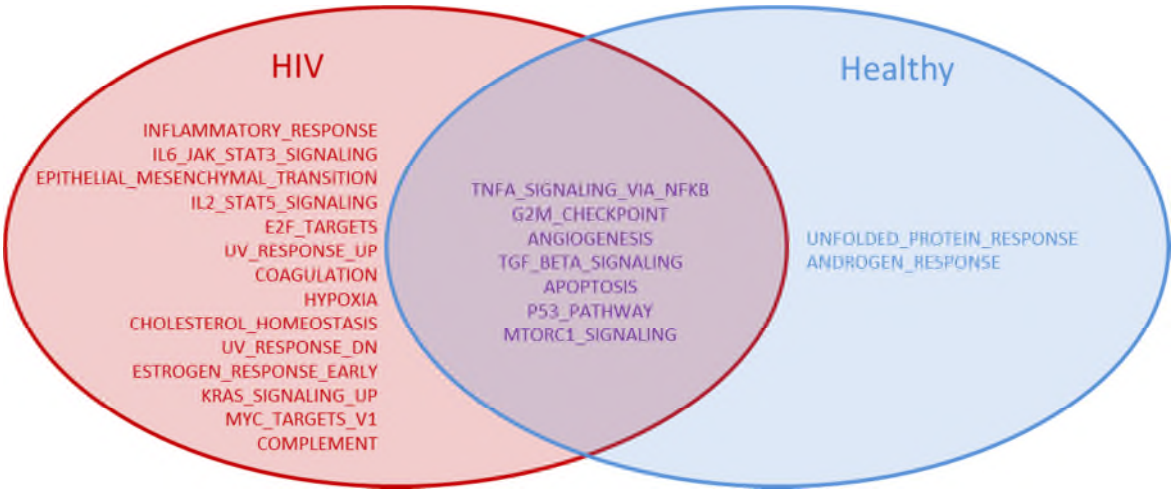

Figure 7. GSEA gene sets significantly affected by HAART. Venn chat shows HAART upregulated pathways uniquely detected in HIV patients (left) and HIV negative volunteers (right) or shared by both (middle).

4. Discussion

Metabolic abnormalities and systemic immune dysfunctions are common during HIV infection and/or

antiretroviral therapy. Although some transcriptomic studies of HIV infection have revealed global changes in the mRNA and microRNA expression profiles [11, 34, 38, 39], the molecular mechanisms that contribute to these dysfunctions have remained elusive, and the relationship between the PBMC transcriptomic profiles and the differential responses to antiretroviral therapy has been limited for HIV patients. Using transcriptomic analysis based on RNA-Seq, we identified a number of transcriptional features and specific genes that may contribute to the HIV associated dysfunction *in vivo* and provided further insights into the molecular mechanisms of antiretroviral therapy effects on HIV patients.

The differentially expressed genes (DEGs) significantly differed among the five individual subjects (Fig. 2A). H1, who was a healthy volunteer, only expressed 13 HAART down-regulated and 28 up-regulated genes, showing that HAART may only minimally affect the PBMC gene expressions in a healthy person. Despite of the inter-individual variations, 25 DEGs shared by the three HIV patients were identified, demonstrating the power of the comparative transcriptome analyses. Among the 11 HAART-down-regulated genes, the relevance of nine had already been reported in HIV infection (*CD160, CD244, SIGLEC1, IFIT1, IFI44, IFI27, CX3CR1*, *IFI44L* and *MX1*). These genes could directly interact with HIV, take part in immune activation and participate in host defenses that partially control infection (Supplementary Tables S2 & S3). For example, CD160 and CD244 are negative surface receptors expressed on NK cells and activated T cells [21, 40]. The co-expression of multiple distinct inhibitory receptors is associated with greater T cell exhaustion and rapid HIV disease progression [40]. HIV exploits the effects of the molecular immune inhibitory response to facilitate the virus's escape under the surveillance of the immune system [41]. Several studies found that the suppression of HIV replication by antiretroviral therapy could reduce the surface expression of inhibitory molecules on HIV-specific immune cells [4-7], which was also supported by our results.

Four of our detected HAART down-regulated genes (*IFIT1, IFI44, IFI27* and *Mx1*) belong to the

interferon (IFN) inducible gene family and are related to immune activation and immune defenses. After HIV infection, interferon signaling leads to the induction of IFN-stimulated gene (ISGs) expression, which results in the diverse effects of IFNs, including anti-viral replication, immune modulation and antitumor activity. Previous array studies documented that both HIV-1 infection and viral proteins increased the expression of IFN-inducible genes, and ART efficiently mitigated aberrant gene expression [14, 42-44]. Most prominently, *MxA(Mx1)*, a known interferon-induced restriction factor for a diverse range of viruses, may represent a valuable marker to monitor the clinical response to therapy in HIV patients because the levels of serum interferon-alpha and *MxA* mRNA were significantly higher in HIV-infected patients with low CD4 T-cell counts, and the expression of *MxA* directly correlated with HIV RNA copy numbers [45]. Clinical trials also showed that the CD4 T-cell count increased and the HIV-induced cytokine IFN-alpha and its downstream effector *MxA* decreased in the plasma of HIV patients after seven years of antiviral treatment [46].

CX3CR1 is a co-receptor for HIV-1, and some variations increases the susceptibility to HIV-1 infection and rapid progression to AIDS [47]. SIGLEC1 (CD169), which is expressed on IFN-induced monocytes, binds HIV-1 and enhances infectivity [48]. These two factors, which are up-regulated after HIV-1 infection and increase during disease progression [49], directly interact with HIV and may be potential molecular targets associated with the inhibition of virus spread [50]. Li *et al.* [51] proposed a disease model in which the host rapidly responds to HIV-1 infection by increasing the expression of a large number of genes related to the innate and adaptive defenses after HIV infection. The suppression of viral replication by HAART would relieve the stimulus from HIV， thus leading to the decreased expression of these genes [52]. Our results support these previous reports, which demonstrate that the comparative transcriptome approach can efficiently extract valuable information from a large number of detected genes using a small sample set, i.e. samples from three HIV-patients and two HIV negative volunteers.

Two genes (*PATL2* and *RASSF1*), whose relationship to HIV infection had not previously been reported, were identified in this study. Although *PATL2* and *RASSF1* have been implicated in cell division and tumor suppression, respectively [53-55], their patterns of down-regulation were similar in the three HIV patients during HAART, as judged by RNA-Seq (Fig. 3B) and qRT-PCR (Fig. 5). This finding suggested that the production of PATL2 and RASSF1 increased during the HIV infection before treatment. Because all three HIV patients shared these two DEGs despite the tremendous inter-individual variations (Figs. 1, 2, and 3A; Supplementary Fig.S1), HIV infection likely resulted in the over-expressions of PATL2 and RASSF1. Therefore, further investigations to determine the relationships of these two proteins with HIV pathogenesis will be worthwhile for treatment development.

Fourteen genes (*ACSL1, GPR84, CXCL1, ADM, S100P, AQP9, GPR97, BASP1, MMP9, SOD2, LRG1, LIMK2, IL1R2* and *BCL2A1*) were up-regulated by HAART in HIV patients compared with the healthy controls. It is worth to note that HAART up-regulation indicated HIV down-regulation but was not correlated to CD4+ cell enrichment in these samples. Based on the commonly accepted notion that there is no “signature genes” in CD4+ cells [56], up-regulations of the genes mentioned above should not be due to the increase of CD4+ cells. Indeed, the CD4+ cell counts did not increase (less than half-fold in P2 and P3, Table 1) proportionally to the RKPM changes (Supplementary Table S4) indicating that the DEGs we recorded (with more than two-fold RKPM change) were not largely due to the increase of CD4+ cell counts although contributions of the CD4+ cells could not be ruled out completely. Therefore, it was mainly the HIV infection that suppressed the expressions of these genes. The relationships of the majority of these genes (9 out 14) with HIV infection had already been reported (Supplementary Table S3). Interestingly, some of the five new genes (*ACSL1, ADM, GPR84, GPR97* and *LRG1*) play key roles in fatty acid metabolism, cell cycle arrest and immunological dysfunction (Fig. 6). For example, GPR97 is an orphan adhesion protein-coupled receptor that binds to chemokines on the surfaces of immune cells. GPR97 has

been suggested to regulate the migration of lymphatic endothelial cells [57] and B-cell development [58], but it has not yet been specifically associated with the host immune responses to a virus. The up-regulation of *GPR97* by HAART suggests that HIV may interfere with some G-protein coupled receptors that are relevant to chemokine signaling pathways, which may be critical for effective antiviral immune responses.

Cardiovascular disease (CVD) has emerged as one of most critical complications of HIV infection. Several clinical studies demonstrated that the rates of CVD among HIV-infected patients were approximately 1.5–2-fold higher than uninfected controls [59-62]. However, the cause of HIV contributing to an increased risk of CVD is still unclear. It has been suggested that HIV-associated CVD may link to T-cell activation, chronic infection, monocyte and macrophage related inflammation and dysfunctional immune regulatory responses [63-69]. We found the up-regulation of *ADM* expression in HIV patients was associated with the decease of HIV load after HAART although ADM had not been reported for association with HIV infection before. ADM has physiological and pathophysiological functions in the cardiovascular system including vasodilation, natriuresis, stimulation of NO production and inhibition of apoptosis [70-72]. ADM also plays a protective role in various pathological conditions including hypertension, myocardial infarction, renal failure and heart failure [73, 74]. As we showed that HAART elevated the level of *ADM* expression in HIV patients but not in HIV negative volunteers, it strongly suggested that HIV infection suppressed the expression of ADM in PBMC. Although direct evidence is needed to clarify the relationship between HIV activity and ADM levels, it is tempting to consider the therapeutic possibility that ADM may be used to treat HIV-associated diseases as ADM is involved in many biological functions (Figs. 6 & 8).

Finally, our work showed that HAART resulted in significant inter-individual variability among DEGs, which reflected the diversity in HIV-affected human gene expressions (Figs. 1-4). These observations also highlighted the importance of determining common as well as personal specific DEG profiles to develop effective diagnostic markers and treatment targets.

5. Conclusions

In this study, we use RNA sequencing (RNA-Seq) technology to identify common DEGs and special DEGs for HIV positive and HIV negative person between pre- and post- HAART. We found 11 down-regulate DEGs and 14 up-regulated DEGs in HIV positive patient. Our work showed that HAART resulted in significant inter-individual variability among DEGs, which reflected the diversity in HIV-affected human gene expressions. The newly identified HIV-related genes, *ADM* (which encodes Adrenomedullin), a peptide hormone in circulation control, may contribute to HIV-associated hypertensions, providing new insights into HIV pathology and novel strategies for developing anti-HIV target. These observations also highlighted the importance of determining common as well as personal specific DEG profiles to develop effective diagnostic markers and treatment targets.

Acknowledgments

This study was supported by grants from the Ministry of Science and Technology of the People's Republic of China (China, grant no. 2011DFA33220), the Key Program of the Natural Science Foundation of Guangdong Province, China (S2012020010873), the Science and Technology Innovation Foundation of Shenzhen, China (CYJ20120829093552348&JCYJ20150402111430645) and the Shenzhen Key Fund for Emerging Infectious Diseases (201506048).

Author Contributions Statement

Y.L. and H.W. designed the work; Y.D. isolated PBMC and extraction RNA; L.H. did RNA-Seq sequencing; F.Z.,J.M. and L.L analyzed experimental results and interpreted the data; S.L. and Y.Z collected samples; J.L. and H.J. did qRT-PCR; F.X. and Y.H. assisted with analysis of the DEG; S.G did Gene Set Enrichment Analysis (GSEA); F.Z. and J.M. wrote the manuscript; Y.L. and H.W. revised it critically; H.Y. gave important suggestions and help revising the manuscript.

References

[1] P.R. Clapham, A. McKnight, HIV-1 receptors and cell tropism, British medical bulletin, 58 (2001) 43-59.

[2] R.S. Veazey, M. DeMaria, L.V. Chalifoux, D.E. Shvetz, D.R. Pauley, H.L. Knight, M. Rosenzweig, R.P. Johnson, R.C. Desrosiers, A.A. Lackner, Gastrointestinal tract as a major site of CD4+ T cell depletion and viral replication in SIV infection, Science, 280 (1998) 427-431.

[3] D. Guha, V. Ayyavoo, Innate Immune Evasion Strategies by Human Immunodeficiency Virus Type 1, Isrn Aids, 2013 (2013) 954806.

[4] A. Sivro, R.C. Su, F.A. Plummer, T.B. Ball, Interferon responses in HIV infection: from protection to disease, AIDS reviews, 16 (2014) 43-51.

[5] L. Zhang, B. Ramratnam, K. Tenner-Racz, Y. He, M. Vesanen, S. Lewin, A. Talal, P. Racz, A.S. Perelson, B.T. Korber, M. Markowitz, D.D. Ho, Quantifying residual HIV-1 replication in patients receiving combination antiretroviral therapy, The New England journal of medicine, 340 (1999) 1605-1613.

[6] F.J. Mateen, S. Kanters, R. Kalyesubula, B. Mukasa, E. Kawuma, A.P. Kengne, E.J. Mills, Hypertension prevalence and Framingham risk score stratification in a large HIV-positive cohort in Uganda, Journal of hypertension, 31 (2013) 1372-1378; discussion 1378.

[7] F.J. Palella, Jr., J.P. Phair, Cardiovascular disease in HIV infection, Current opinion in HIV and AIDS, 6 (2011) 266-271.

[8] M. Muller, S. Wandel, R. Colebunders, S. Attia, H. Furrer, M. Egger, D.E.A.S. Ie, A. Central, Immune reconstitution inflammatory syndrome in patients starting antiretroviral therapy for HIV infection: a systematic review and meta-analysis, The Lancet infectious diseases, 10 (2010) 251-261.

[9] K.C. Chan, R.A. Galli, J.S. Montaner, P.R. Harrigan, Prolonged retention of drug resistance mutations and rapid disease progression in the absence of therapy after primary HIV infection, AIDS, 17 (2003) 1256-1258.

[10] D. Chaussabel, V. Pascual, J. Banchereau, Assessing the human immune system through blood transcriptomics, BMC biology, 8 (2010) 84.

[11] M.B. Ryndak, K.K. Singh, Z. Peng, S. Zolla-Pazner, H. Li, L. Meng, S. Laal, Transcriptional Profiling of Mycobacterium tuberculosis Replicating Ex vivo in Blood from HIV- and HIV+ Subjects, PloS one, 9 (2014) e94939.

[12] J.Q. Wu, T.R. Sasse, G. Wolkenstein, V. Conceicao, M.M. Saksena, M. Soedjono, S.S. Perera, B. Wang, D.E. Dwyer, N.K. Saksena, Transcriptome analysis of primary monocytes shows global down-regulation of genetic networks in HIV viremic patients versus long-term non-progressors, Virology, 435 (2013) 308-319.

[13] M.S. Giri, M. Nebozhyn, L. Showe, L.J. Montaner, Microarray data on gene modulation by HIV-1 in immune cells: 2000-2006, Journal of leukocyte biology, 80 (2006) 1031-1043.

[14] V.N. da Conceicao, W.B. Dyer, K. Gandhi, P. Gupta, N.K. Saksena, Genome-wide analysis of primary peripheral blood mononuclear cells from HIV + patients-pre-and post- HAART show immune activation and inflammation the main drivers of host gene expression, Molecular and cellular therapies, 2 (2014) 11.

[15] M. Rotger, K.K. Dang, J. Fellay, E.L. Heinzen, S. Feng, P. Descombes, K.V. Shianna, D. Ge, H.F. Gunthard, D.B. Goldstein, A. Telenti, Genome-wide mRNA expression correlates of viral control in CD4+ T-cells from HIV-1-infected individuals, PLoS pathogens, 6 (2010) e1000781.

[16] M.L. Metzker, Sequencing technologies - the next generation, Nature reviews. Genetics, 11 (2010) 31-46.

[17] U. Nagalakshmi, K. Waern, M. Snyder, RNA-Seq: a method for comprehensive transcriptome analysis, Current protocols in molecular biology / edited by Frederick M. Ausubel ... [et al.], Chapter 4 (2010) Unit 4 11 11-13.

[18] Z. Wang, M. Gerstein, M. Snyder, RNA-Seq: a revolutionary tool for transcriptomics, Nature reviews. Genetics, 10 (2009) 57-63.

[19] M.L. Yeung, Y. Bennasser, K. Watashi, S.Y. Le, L. Houzet, K.T. Jeang, Pyrosequencing of small non-coding RNAs in HIV-1 infected cells: evidence for the processing of a viral-cellular double-stranded RNA hybrid, Nucleic acids research, 37 (2009) 6575-6586.

[20] Y. Pacheco, A.P. McLean, J. Rohrbach, F. Porichis, D.E. Kaufmann, D.G. Kavanagh, Simultaneous TCR and CD244 signals induce dynamic downmodulation of CD244 on human antiviral T cells, J Immunol, 191 (2013) 2072-2081.

[21] S.R. Ostrowski, H. Ullum, B.K. Pedersen, J. Gerstoft, T.L. Katzenstein, 2B4 expression on natural killer cells increases in HIV-1 infected patients followed prospectively during highly active antiretroviral therapy, Clinical and experimental immunology, 141 (2005) 526-533.
[22] T. Yamamoto, D.A. Price, J.P. Casazza, G. Ferrari, M. Nason, P.K. Chattopadhyay, M. Roederer, E. Gostick, P.D. Katsikis, D.C. Douek, R. Haubrich, C. Petrovas, R.A. Koup, Surface expression patterns of negative regulatory molecules identify determinants of virus-specific CD8+ T-cell exhaustion in HIV infection, Blood, 117 (2011) 4805-4815.
[23] N.C. Twine, J.A. Stover, B. Marshall, G. Dukart, M. Hidalgo, W. Stadler, T. Logan, J. Dutcher, G. Hudes, A.J. Dorner, D.K. Slonim, W.L. Trepicchio, M.E. Burczynski, Disease-associated expression profiles in peripheral blood mononuclear cells from patients with advanced renal cell carcinoma, Cancer research, 63 (2003) 6069-6075.
[24] M.K. Showe, A. Vachani, A.V. Kossenkov, M. Yousef, C. Nichols, E.V. Nikonova, C. Chang, J. Kucharczuk, B. Tran, E. Wakeam, T.A. Yie, D. Speicher, W.N. Rom, S. Albelda, L.C. Showe, Gene expression profiles in peripheral blood mononuclear cells can distinguish patients with non-small cell lung cancer from patients with nonmalignant lung disease, Cancer research, 69 (2009) 9202-9210.
[25] K. Pecankova, P. Majek, J. Cermak, J.E. Dyr, Peripheral blood mononuclear cell proteome changes in patients with myelodysplastic syndrome, BioMed research international, 2015 (2015) 872983.
[26] WHO., Treatment of Tuberculosis: guidelines for national programmes.http://whqlibdoc.who.int/publications/2010/9789241547833_eng.pdf?ua=1 (accessed Oct 26, 2014), in.
[27] Z. Fujie, China Free Antiretroviral Therapy Manual, 2012 edn.
[28] Z. Zhao, J. Xu, J. Chen, S. Kim, M. Reimers, S.A. Bacanu, H. Yu, C. Liu, J. Sun, Q. Wang, P. Jia, F. Xu, Y. Zhang, K.S. Kendler, Z. Peng, X. Chen, Transcriptome sequencing and genome-wide association analyses reveal lysosomal function and actin cytoskeleton remodeling in schizophrenia and bipolar disorder, Molecular psychiatry, (2014).
[29] R. Li, C. Yu, Y. Li, T.W. Lam, S.M. Yiu, K. Kristiansen, J. Wang, SOAP2: an improved ultrafast tool for short read alignment, Bioinformatics, 25 (2009) 1966-1967.
[30] S. Tarazona, F. Garcia-Alcalde, J. Dopazo, A. Ferrer, A. Conesa, Differential expression in RNA-seq: a matter of depth, Genome research, 21 (2011) 2213-2223.
[31] W. Huang da, B.T. Sherman, R.A. Lempicki, Systematic and integrative analysis of large gene lists using DAVID bioinformatics resources, Nature protocols, 4 (2009) 44-57.
[32] A. Subramanian, P. Tamayo, V.K. Mootha, S. Mukherjee, B.L. Ebert, M.A. Gillette, A. Paulovich, S.L. Pomeroy, T.R. Golub, E.S. Lander, J.P. Mesirov, Gene set enrichment analysis: a knowledge-based approach for interpreting genome-wide expression profiles, Proceedings of the National Academy of Sciences of the United States of America, 102 (2005) 15545-15550.
[33] T. Nolan, R.E. Hands, S.A. Bustin, Quantification of mRNA using real-time RT-PCR, Nature protocols, 1 (2006) 1559-1582.
[34] J.Q. Wu, T.R. Sasse, M.M. Saksena, N.K. Saksena, Transcriptome analysis of primary monocytes from HIV-positive patients with differential responses to antiretroviral therapy, Virology journal, 10 (2013) 361.
[35] M.L. Wong, J.F. Medrano, Real-time PCR for mRNA quantitation, BioTechniques, 39 (2005) 75-85.
[36] O. Benga, V.J. Huber, Brain water channel proteins in health and disease, Molecular aspects of medicine, 33 (2012) 562-578.
[37] C. Demacq, V.B. Vasconcellos, A.M. Marcaccini, R.F. Gerlach, A.A. Machado, J.E. Tanus-Santos, A genetic polymorphism of matrix metalloproteinase 9 (MMP-9) affects the changes in circulating MMP-9 levels induced by highly active antiretroviral therapy in HIV patients, The pharmacogenomics journal, 9 (2009) 265-273.
[38] H.T. Tran, R. Van den Bergh, T.N. Vu, K. Laukens, W. Worodria, M.M. Loembe, R. Colebunders, L. Kestens, P. De Baetselier, G. Raes, The role of monocytes in the development of Tuberculosis-associated Immune Reconstitution Inflammatory Syndrome, Immunobiology, 219 (2014) 37-44.
[39] Z.N. Zhang, J.J. Xu, Y.J. Fu, J. Liu, Y.J. Jiang, H.L. Cui, B. Zhao, H. Sun, Y.W. He, Q.J. Li, H. Shang, Transcriptomic analysis of peripheral blood mononuclear cells in rapid progressors in early HIV infection identifies a signature closely correlated with disease progression, Clinical chemistry, 59 (2013) 1175-1186.
[40] M. Larsson, E.M. Shankar, K.F. Che, A. Saeidi, R. Ellegard, M. Barathan, V. Velu, A. Kamarulzaman, Molecular signatures of T-cell inhibition in HIV-1 infection, Retrovirology, 10 (2013) 31.
[41] K.N. Aldy, N.C. Horton, P.A. Mathew, S.O. Mathew, 2B4+ CD8+ T cells play an inhibitory role against constrained HIV epitopes, Biochemical and biophysical research communications, 405 (2011) 503-507.

649 [42] S.H. Wie, P. Du, T.Q. Luong, S.E. Rought, N. Beliakova-Bethell, J. Lozach, J. Corbeil, R.S. Kornbluth, D.D. Richman, C.H. Woelk,
650 HIV downregulates interferon-stimulated genes in primary macrophages, Journal of interferon & cytokine research : the official
651 journal of the International Society for Interferon and Cytokine Research, 33 (2013) 90-95.
652 [43] E. Izmailova, F.M. Bertley, Q. Huang, N. Makori, C.J. Miller, R.A. Young, A. Aldovini, HIV-1 Tat reprograms immature dendritic
653 cells to express chemoattractants for activated T cells and macrophages, Nature medicine, 9 (2003) 191-197.
654 [44] A. Borjabad, S. Morgello, W. Chao, S.Y. Kim, A.I. Brooks, J. Murray, M.J. Potash, D.J. Volsky, Significant effects of antiretroviral
655 therapy on global gene expression in brain tissues of patients with HIV-1-associated neurocognitive disorders, PLoS pathogens, 7
656 (2011) e1002213.
657 [45] R. Badolato, C. Ghidini, F. Facchetti, F. Serana, A. Sottini, M. Chiarini, E. Spinelli, S. Lonardi, A. Plebani, L. Caimi, L. Imberti,
658 Type I interferon-dependent gene MxA in perinatal HIV-infected patients under antiretroviral therapy as marker for therapy
659 failure and blood plasmacytoid dendritic cells depletion, Journal of translational medicine, 6 (2008) 49.
660 [46] N. Jung, C. Lehmann, M. Knispel, E.K. Meuer, J. Fischer, G. Fatkenheuer, P. Hartmann, D. Taubert, Long-term beneficial effect
661 of protease inhibitors on the intrinsic apoptosis of peripheral blood mononuclear cells in HIV-infected patients, HIV medicine, 13
662 (2012) 469-478.
663 [47] Y. Becker, The spreading of HIV-1 infection in the human organism is caused by fractalkine trafficking of the infected
664 lymphocytes--a review, hypothesis and implications for treatment, Virus genes, 34 (2007) 93-109.
665 [48] A.C. van der Kuyl, R. van den Burg, F. Zorgdrager, F. Groot, B. Berkhout, M. Cornelissen, Sialoadhesin (CD169) expression in
666 CD14+ cells is upregulated early after HIV-1 infection and increases during disease progression, PloS one, 2 (2007) e257.
667 [49] S. Krishnan, E.M. Wilson, V. Sheikh, A. Rupert, D. Mendoza, J. Yang, R. Lempicki, S.A. Migueles, I. Sereti, Evidence for innate
668 immune system activation in HIV type 1-infected elite controllers, The Journal of infectious diseases, 209 (2014) 931-939.
669 [50] X. Yu, A. Feizpour, N.G. Ramirez, L. Wu, H. Akiyama, F. Xu, S. Gummuluru, B.M. Reinhard, Glycosphingolipid-functionalized
670 nanoparticles recapitulate CD169-dependent HIV-1 uptake and trafficking in dendritic cells, Nature communications, 5 (2014)
671 4136.
672 [51] Q. Li, T. Schacker, J. Carlis, G. Beilman, P. Nguyen, A.T. Haase, Functional genomic analysis of the response of HIV-1-infected
673 lymphatic tissue to antiretroviral therapy, The Journal of infectious diseases, 189 (2004) 572-582.
674 [52] Q. Li, A.J. Smith, T.W. Schacker, J.V. Carlis, L. Duan, C.S. Reilly, A.T. Haase, Microarray analysis of lymphatic tissue reveals
675 stage-specific, gene expression signatures in HIV-1 infection, J Immunol, 183 (2009) 1975-1982.
676 [53] N. Scheller, P. Resa-Infante, S. de la Luna, R.P. Galao, M. Albrecht, L. Kaestner, P. Lipp, T. Lengauer, A. Meyerhans, J. Diez,
677 Identification of PatL1, a human homolog to yeast P body component Pat1, Biochimica et biophysica acta, 1773 (2007)
678 1786-1792.
679 [54] M.I. Rather, S. Swamy, K.S. Gopinath, A. Kumar, Transcriptional repression of tumor suppressor CDC73, encoding an RNA
680 polymerase II interactor, by Wilms tumor 1 protein (WT1) promotes cell proliferation: implication for cancer therapeutics, The
681 Journal of biological chemistry, 289 (2014) 968-976.
682 [55] L. Liu, V. Amy, G. Liu, W.L. McKeehan, Novel complex integrating mitochondria and the microtubular cytoskeleton with
683 chromosome remodeling and tumor suppressor RASSF1 deduced by in silico homology analysis, interaction cloning in yeast, and
684 colocalization in cultured cells, In vitro cellular & developmental biology. Animal, 38 (2002) 582-594.
685 [56] C. Palmer, M. Diehn, A.A. Alizadeh, P.O. Brown, Cell-type specific gene expression profiles of leukocytes in human peripheral
686 blood, BMC genomics, 7 (2006) 115.
687 [57] N. Valtcheva, A. Primorac, G. Jurisic, M. Hollmen, M. Detmar, The orphan adhesion G protein-coupled receptor GPR97
688 regulates migration of lymphatic endothelial cells via the small GTPases RhoA and Cdc42, The Journal of biological chemistry, 288
689 (2013) 35736-35748.
690 [58] J.J. Wang, L.L. Zhang, H.X. Zhang, C.L. Shen, S.Y. Lu, Y. Kuang, Y.H. Wan, W.G. Wang, H.M. Yan, S.Y. Dang, J. Fei, X.L. Jin, Z.G.
691 Wang, Gpr97 is essential for the follicular versus marginal zone B-lymphocyte fate decision, Cell death & disease, 4 (2013) e853.
692 [59] V.A. Triant, H. Lee, C. Hadigan, S.K. Grinspoon, Increased acute myocardial infarction rates and cardiovascular risk factors
693 among patients with human immunodeficiency virus disease, The Journal of clinical endocrinology and metabolism, 92 (2007)
694 2506-2512.
695 [60] N. Obel, H.F. Thomsen, G. Kronborg, C.S. Larsen, P.R. Hildebrandt, H.T. Sorensen, J. Gerstoft, Ischemic heart disease in

HIV-infected and HIV-uninfected individuals: a population-based cohort study, Clinical infectious diseases : an official publication of the Infectious Diseases Society of America, 44 (2007) 1625-1631.
[61] S. Lang, M. Mary-Krause, L. Cotte, J. Gilquin, M. Partisani, A. Simon, F. Boccara, A. Bingham, D. Costagliola, Increased risk of myocardial infarction in HIV-infected patients in France, relative to the general population, Aids, 24 (2010) 1228-1230.
[62] D.B. Klein, W.A. Leyden, L. Xu, C.R. Chao, M.A. Horberg, W.J. Towner, L.B. Hurley, J.L. Marcus, C.P. Quesenberry, Jr., M.J. Silverberg, Declining relative risk for myocardial infarction among HIV-positive compared with HIV-negative individuals with access to care, Clinical infectious diseases : an official publication of the Infectious Diseases Society of America, 60 (2015) 1278-1280.
[63] P.Y. Hsue, P.W. Hunt, E. Sinclair, B. Bredt, A. Franklin, M. Killian, R. Hoh, J.N. Martin, J.M. McCune, D.D. Waters, S.G. Deeks, Increased carotid intima-media thickness in HIV patients is associated with increased cytomegalovirus-specific T-cell responses, Aids, 20 (2006) 2275-2283.
[64] P.M. Ridker, N. Rifai, L. Rose, J.E. Buring, N.R. Cook, Comparison of C-reactive protein and low-density lipoprotein cholesterol levels in the prediction of first cardiovascular events, The New England journal of medicine, 347 (2002) 1557-1565.
[65] R.S. Baliga, A.A. Chaves, L. Jing, L.W. Ayers, J.A. Bauer, AIDS-related vasculopathy: evidence for oxidative and inflammatory pathways in murine and human AIDS, American journal of physiology. Heart and circulatory physiology, 289 (2005) H1373-1380.
[66] C.M. Shikuma, L.J. Day, M. Gerschenson, Insulin resistance in the HIV-infected population: the potential role of mitochondrial dysfunction, Current drug targets. Infectious disorders, 5 (2005) 255-262.
[67] M. Troseid, I.W. Manner, K.K. Pedersen, J.M. Haissman, D. Kvale, S.D. Nielsen, Microbial translocation and cardiometabolic risk factors in HIV infection, AIDS research and human retroviruses, 30 (2014) 514-522.
[68] V.A. Triant, S. Regan, H. Lee, P.E. Sax, J.B. Meigs, S.K. Grinspoon, Association of immunologic and virologic factors with myocardial infarction rates in a US healthcare system, Journal of acquired immune deficiency syndromes, 55 (2010) 615-619.
[69] S. Lang, M. Mary-Krause, A. Simon, M. Partisani, J. Gilquin, L. Cotte, F. Boccara, D. Costagliola, HIV replication and immune status are independent predictors of the risk of myocardial infarction in HIV-infected individuals, Clinical infectious diseases : an official publication of the Infectious Diseases Society of America, 55 (2012) 600-607.
[70] A. Funke-Kaiser, A.S. Havulinna, T. Zeller, S. Appelbaum, P. Jousilahti, E. Vartiainen, S. Blankenberg, K. Sydow, V. Salomaa, Predictive value of midregional pro-adrenomedullin compared to natriuretic peptides for incident cardiovascular disease and heart failure in the population-based FINRISK 1997 cohort, Annals of medicine, 46 (2014) 155-162.
[71] T. Nishikimi, K. Kuwahara, Y. Nakagawa, K. Kangawa, K. Nakao, Adrenomedullin in cardiovascular disease: a useful biomarker, its pathological roles and therapeutic application, Current protein & peptide science, 14 (2013) 256-267.
[72] M. Sata, M. Kakoki, D. Nagata, H. Nishimatsu, E. Suzuki, T. Aoyagi, S. Sugiura, H. Kojima, T. Nagano, K. Kangawa, H. Matsuo, M. Omata, R. Nagai, Y. Hirata, Adrenomedullin and nitric oxide inhibit human endothelial cell apoptosis via a cyclic GMP-independent mechanism, Hypertension, 36 (2000) 83-88.
[73] H.K. Wong, T.T. Cheung, B.M. Cheung, Adrenomedullin and cardiovascular diseases, JRSM cardiovascular disease, 1 (2012).
[74] D. Holmes, M. Campbell, M. Harbinson, D. Bell, Protective effects of intermedin on cardiovascular, pulmonary and renal diseases: comparison with adrenomedullin and CGRP, Current protein & peptide science, 14 (2013) 294-329.

Supporting Information

Supplementary Table S1: The summary of sequencing datasets

Supplementary Table S2: Table S1: All primer sequences for qRT-PCR verification

Supplementary Table S3: HAART down-regulated genes

Supplementary Table S4: HAART up-regulated genes

Supplementary Table S5: Quantitative real time PCR validations of differentially expressed genes

Supplementary Table S6: Gene Ontology Enrichment Table

Supplementary Table S7: Different express genes between control and patient group before HARRT. The red color highlighted genes were down-regulated genes in patients after HARRT and the yellow highlighted genes were up-regulated genes in patients after HARRT.

Supplementary Fig. S1: Global gene expression plot of individual HIV patients and HIV-negative volunteers. Each panel represents samples from an individual (HIV negative volunteers, H1 & H2; HIV patients, P1-3). The X-axis represents RKPM values of Post-HAART while the Y-axis represents RKPM of Pre-HAART. All qualified genes are represented. The blue dots are DEGs detected in each individual. The red labels are DEGs selected for experimental (qRT-PCR) validation and the yellow labels are the novel HIV-relevant genes detected in this study.

Supplementary Fig. S2: The highlight relationship of newly report HIV-related genes for GO terms and GSEA pathways.

Supplementary Table S1. The summary of sequencing datasets

Sample ID	Total Reads (M)	Total Base Pairs (G)	Total Mapped (%)*	Perfect Match (%)**	Unique Match (%)**
P1-0W ****	59.61	5.36	80.40	64.75	73.53
P1-2W	59.64	5.37	80.35	64.30	76.28
P2-0W	59.52	5.36	75.68	60.14	73.71
P2-2W	59.75	5.38	73.66	58.56	71.69
P3-0W	59.73	5.38	77.69	62.24	75.41
P3-2W	59.13	5.32	75.11	60.13	72.50
H1-0W	46.26	4.16	81.92	65.47	79.50
H1-2W	59.32	5.34	80.73	64.69	78.61
H2-0W	58.88	5.30	75.33	60.84	68.16
H2-2W	58.74	5.29	75.47	60.20	68.39

* Reads were mapped against human reference sequence

** Reads perfectly matched to the human reference sequence

*** Reads uniquely matched to a single location in the human reference sequence

**** 0W denotes pre-HAART and 2W denotes 2 weeks after HAART started

Table S1: All primer sequences for qRT-PCR verification

Name	Sequence	Name
ACSL1	Forward primer: AGGATTTGAAGGGTCGTTTG Reverse primer: TAATTCAGGGTGCAATGTGAT	CD160
GPR84	Forward primer: TACACCGCCAGGTCAAACG Reverse primer: ACTGGGTCCTCCTGATGCTAA	CD244
ADM	Forward primer: CGAGTGTTTGCCAGGCTTAA Reverse primer: GCGTGAGAAATCAGTTTGTGG	IFIT1
S100P	Forward primer: ACACGCAGACCCTGACCAA Reverse primer: CAGCCACGAACACGATGAAC	IFI44
AQP9	Forward primer: TCCAGTTCCCGCTATGCT Reverse primer: GAATGCCACAATGTCCTCC	IFI44L
GPR97	Forward primer: CAGAGATACTGGCTAAACTACG Reverse primer: TCTCTTGGGAAGTCGCAC	IFI27
BASP1	Forward primer:TAGCACCCAGAGCCGAACT Reverse primer: AGGCTTTCTCGTCGTTCACA	Mx1
MMP9	Forward primer: CAGGCGCTCATGTACCCTA Reverse primer: TCAGGGCGAGGACCATAGA	CX3CR1
SOD2	Forward primer: TGGAGCACGCTTACTACCTTC Reverse primer:GCAAGCCATGTATCTTTCAGTT	SIGLEC1
LRG1	Forward primer: TTCAACCTGACCCACCTGC Reverse primer: AGGGCGTTTCGGGTTAGAT	PATL2
LIMK2	Forward primer: GGCTGAGAACTTACGGACAACA Reverse primer: GAGCCCACCCGAGTATGAGTA	RASSF1
IL1R2	Forward primer: AGATGCTTTCCTGCCGTT Reverse primer: TCACTCAGGTCAGGGCATAC	RNU2-1
BCL2A1	Forward primer: TGCGTCCTACAGATACCACAA Reverse primer: GTGTTCTGGCAGTGTCTACGG	SFXN1
CXCL1	Forward primer:TCAGAAGGGAGGAGGAAGC Reverse primer: CTCCTAAGCGATGCTCAAACA	SOCS3
		CDKN1C

Sequence
Forward primer: CACAGTGACGGGATTGAAACA
Reverse primer: GGTGACCAGCATTACCCAGAC
Forward primer: CACCTAAAGCCCAGAACCCT
Reverse primer: AACTCCTGTGCCGTCATCC
Forward primer: GCTCAAATCCCTTCCGCTAT
Reverse primer: TTCCAGGCGATAGGCAGAG
Forward primer: TCCCTGGTTCAACAAATACGA
Reverse primer: TATGCCCACCAAAGCCTGA
Forward primer: ACAGAGCCAAATGATTCCCTATG
Reverse primer: TCGATAAACGACACACCAGTTG
Forward primer: TGCTCTCACCTCATCAGCAGT
Reverse primer: CACAACTCCTCCAATCACAACT
Forward primer: GGTGGTCCCCAGTAATGTGG
Reverse primer: CGTCAAGATTCCGATGGTCCT
Forward primer: GCTCTTCTGGACACCCTACAAC
Reverse primer:CTCAGGCAACAATGGCTAAAT
Forward primer: CCACTAGGGCTGATACTGGCT
Reverse primer: GAGGCGGGTGGTTGACTAC
Forward primer: GAGGCTTATGAGTCCGTGGTC
Reverse primer: ACTTCCAGCCTTCCTCTATTTC
Forward primer: TAGGGTGGGTGCTCAGAATAA
Reverse primer: AACCAGCACTCCCTGACCT
Forward primer: GCCTTTTGGCTAAGATCAAGT
Reverse primer: TACTGCAATACCAGGTCGATG
Forward primer:AAGTTGGCATTCCCGTCAC
Reverse primer: GAGAATCCTGGACACGACAAC
Forward primer: GAGTTCCTGGACCAGTACGATG
Reverse primer: TCTGGTTGGCTTCTTGTGCT
Forward primer: CCAAAGGCACTCTCCATCTC
Reverse primer: GCTAGATGGGCATGTATGGC

Table.S3: Eleven down-regulated DEGs in HIV infected patients, one down-regulated DEGs in HIV/TB co-infected patients and one down-regulated DEGs in healthy controls by antiretroviral therapy.

Gene ID	Gene symbol	full_name	function descripton	RefSeq Accession	HIV relevant studies	Reference
11126	CD160	CD160 molecule	negative regulator of T cell activation	NM_007053	CD160 was up-regulated on HIV-specific CD8 T lymphocytes mostly during the chronic phase of infection.	[1-4]
51744	CD244	natural killer cell receptor 2B4	modulate NK-cell cytolytic activity and inhibitory receptor in CD8+ T cells	NM_016382	2B4 expression on natural killer cells increases in HIV-1 infected patients	[5-7]
3434	IFIT1	Interferon-Induced Protein With Tetratricopeptide Repeats 1	inhibit viral replication and translational initiation	NM_001548	HIV infection induces the expression of IFIT1.	[8-11]
10561	IFI44	interferon-induced protein 44	Antiproliferative activity and inhibit viral replication	NM_006417	HIV-1 infection or Tat expression induces interferon (IFN)-responsive gene expression（IFI44,IFI27，MX1)	[8, 9, 12-14]
10964	IFI44L	interferon-induced protein 44-like	immune defense response to virus	NM_006820	HIV-1 gp120-treated vaginal epithelial cells show upregulation of IFI44Lexpression	[15]
3429	IFI27	interferon, alpha-inducible protein 27	inhibit viral replication and enhances the immune response	NM_005532	HIV downregulates interferon-stimulated genes in primary macrophages；IFI27 expression in HIV/HCV co-infection.	[12, 16, 17]
4599	Mx1	myxovirus (influenza virus) resistance 1	participates in the cellular antiviral response	NM_002462	Regulation of interferon-alpha-inducible cellular genes in human immunodeficiency virus-infected monocytes	[18-22]
1524	CX3CR1	chemokine (C-X3-C motif) receptor 1	the adhesion and migration of leukocytes	NM_001337	coreceptor for HIV-1 and increased susceptibility to HIV-1 infection and rapid progression to AIDS	[23]
6614	SIGLEC1	sialic acid binding Ig-like lectin 1	mediating cell-cell interactions，Binds HIV-1 and Enhances Infectivity	NM_023068	virus-cell interactions between HIV-1 and Siglec1/CD169, a protein expressed on dendritic cells	[24, 25]
197135	PATL2	protein associated with topoisomerase II homolog 2	RNA binding and protein binding	NM_001145112	No report	
11186	RASSF1	Ras association (RalGDS/AF-6) domain family member 1	the tumor suppressor function and induce cell cycle arrest	NM_170712	No report	
1028	CDKN1C	Cyclin-dependent kinase inhibitor 1C	strong inhibitor of several G1 cyclin/Cdk complexes and a negative regulator of cell proliferation	NM_000076	HIV-1-infected cells lose their G(1)/S checkpoints due to a loss of cycline-dependent kinase inhibitor.	[26]
6066	RNU2-1	RNA, U2 small nuclear 1	a RNA component of the U2 snRNP that interacts with the 3' region of the intron at the branch site	N/A	No report	

Table.S4: Fourteen up-regulated DEGs in HIV-infected patients and two up-regulated DEGs in HIV/TB co-infected patients by antiretroviral therapy

Gene ID	Gene symbol	Full name	function descripton	RefSeq Accession	HIV relevant studies	Reference
2180	ACSL1	acyl-CoA synthetase long-chain family member 1	Activation of long-chain fatty acids for both synthesis of cellular lipids, and degradation via beta-oxidation	NM_001995	No report	
53831	GPR84	G protein-coupled receptor 84	fatty acid metabolism and immunological regulation	NM_020370	No report	
133	ADM	adrenomedullin	a hormone in circulation control	NM_001124	No report	
6286	S100P	S100 calcium binding protein P	the regulation of a number of cellular processes such as cell cycle progression and differentiation	NM_005980	Potential therapeutic targets for HIV infection	[10]
366	AQP9	aquaporin 9	water-selective membrane channels，immunological response and bactericidal activity	NM_020980	Brain water channel proteins involved in HIV-associated dementia and transcription profile of CD4(+) T cells in HIV/HCV co-infection.	[27, 28]
222487	GPR97	G protein-coupled receptor 97	regulating migration of lymphatic endothelial cells and B-cell development	NM_170776	No report	
10409	BASP1	brain abundant, membrane attached signal protein 1	transient phosphorylation sites and PEST motifs	NM_006317	HIV-1 Tat up-regulates the expression of BASP1 in human primary T cells	[29]
4318	MMP9	matrix metallopeptidase 9	breakdown of extracellular matrix，embryonic development, reproduction, and tissue remodeling	NM_004994	MMP-9 activity levels are associated with cardiovascular diseases	[30]
6648	SOD2	superoxide dismutase 2	converts superoxide byproducts of oxidative phosphorylation to hydrogen peroxide and diatomic oxygen.	NM_000636	HIV gp120 regulate SOD2 in HIV-associated dementia.	[31]
116844	LRG1	leucine-rich alpha-2-glycoprotein 1	Protein-protein interaction, signal transduction, and cell adhesion and development.	NM_052972	No report	
3985	LIMK2	LIM domain kinase 2	a TKL kinase of the LISK family that regulates actin dynamics	NM_005569	the RhoA-ROCK-LIMK-cofilin pathway in HIV-1 infection	[32, 33]
7850	IL1R2	interleukin 1 receptor, type II	MAPK signaling pathway and IL1-mediated signaling events	NM_004633	Gene expression profiling of the host response to HIV-1 infection in monocyte-derived dendritic cells	[34]
597	BCL2A1	BCL2-related protein A1(Bfl-1)	anti- and pro-apoptotic regulators	NM_004049	Gp120-induced M-CSF up-regulates the anti-apoptotic genes Bfl-1	[35]
2919	CXCL1	Chemokine (C-X-C motif) ligand 1	Playing a role in inflammation as a chemo-attractant for neutrophils.	NM_001511	Induction of IL-17 and T-cell activation by HIV-Tat protein	[29]
94081	SFXN1	Sideroflexin-1	double-stranded RNA-binding protein	NM_022754	Combine with HIV RNA and form RNP in host cells, participate in the formation of HIV packaging.	[36]

9021	SOCS3	Suppressor of cytokine signaling 3	cytokine-inducible negative regulators of cytokine signaling	NM_003955	HIV-1 Tat upregulates SOCS3 in human primary T cells; HIV-1 gp120 recruits SOCS3 through IL-10 activation.	[29, 37]

Reference

1. Vigano, S., et al., *Rapid perturbation in viremia levels drives increases in functional avidity of HIV-specific CD8 T cells.* PLoS Pathog, 2013. **9**(7): p. e1003423.
2. Peretz, Y., et al., *CD160 and PD-1 co-expression on HIV-specific CD8 T cells defines a subset with advanced dysfunction.* PLoS Pathog, 2012. **8**(8): p. e1002840.
3. Larsson, M., et al., *Molecular signatures of T-cell inhibition in HIV-1 infection.* Retrovirology, 2013. **10**: p. 31.
4. Nikolova, M.H., et al., *The CD160+ CD8high cytotoxic T cell subset correlates with response to HAART in HIV-1+ patients.* Cell Immunol, 2005. **237**(2): p. 96-105.
5. Seung, E., et al., *PD-1 blockade in chronically HIV-1-infected humanized mice suppresses viral loads.* PLoS One, 2013. **8**(10): p. e77780.
6. Pacheco, Y., et al., *Simultaneous TCR and CD244 signals induce dynamic downmodulation of CD244 on human antiviral T cells.* J Immunol, 2013. **191**(5): p. 2072-81.
7. Aldy, K.N., et al., *2B4+ CD8+ T cells play an inhibitory role against constrained HIV epitopes.* Biochem Biophys Res Commun, 2011. **405**(3): p. 503-7.
8. Rempel, H., et al., *Monocyte activation in HIV/HCV coinfection correlates with cognitive impairment.* PLoS One, 2013. **8**(2): p. e55776.
9. Borjabad, A., et al., *Significant effects of antiretroviral therapy on global gene expression in brain tissues of patients with HIV-1-associated neurocognitive disorders.* PLoS Pathog, 2011. **7**(9): p. e1002213.
10. Nguyen, D.G., et al., *Identification of novel therapeutic targets for HIV infection through functional genomic cDNA screening.* Virology, 2007. **362**(1): p. 16-25.
11. Kim, S.Y., et al., *Microarray analysis of changes in cellular gene expression induced by productive infection of primary human astrocytes: implications for HAD.* J Neuroimmunol, 2004. **157**(1-2): p. 17-26.
12. Wie, S.H., et al., *HIV downregulates interferon-stimulated genes in primary macrophages.* J Interferon Cytokine Res, 2013. **33**(2): p. 90-5.
13. Winkler, J.M., A.D. Chaudhuri, and H.S. Fox, *Translating the brain transcriptome in neuroAIDS: from non-human primates to humans.* J Neuroimmune Pharmacol, 2012. **7**(2): p. 372-9.
14. Izmailova, E., et al., *HIV-1 Tat reprograms immature dendritic cells to express chemoattractants for activated T cells and macrophages.* Nat Med, 2003. **9**(2): p. 191-7.
15. Fanibunda, S.E., D.N. Modi, and A.H. Bandivdekar, *HIV gp120 induced gene expression signatures in vaginal epithelial cells.* Microbes Infect, 2013. **15**(12): p. 806-15.
16. Katsounas, A., et al., *Interferon stimulated exonuclease gene 20 kDa links psychiatric events to distinct hepatitis C virus responses in human immunodeficiency virus positive patients.* J Med Virol, 2014. **86**(8): p. 1323-31.
17. Jablonowska, E., et al., *Expression of selected genes in liver biopsy specimens in relation to early virological response in patients with chronic hepatitis C with HCV mono- and HIV/HCV co-infection.* Arch Virol, 2014. **159**(6): p. 1365-71.
18. Monteleone, K., et al., *Interleukin-32 isoforms: expression, interaction with interferon-regulated genes and clinical significance in chronically HIV-1-infected patients.* Med Microbiol Immunol, 2014. **203**(3): p. 207-16.
19. Haller, O., *Dynamins are forever: MxB inhibits HIV-1.* Cell Host Microbe, 2013. **14**(4): p. 371-3.
20. Liu, M.Q., et al., *IFN-lambda3 inhibits HIV infection of macrophages through the JAK-STAT pathway.* PLoS One, 2012. **7**(4): p. e35902.
21. Jung, N., et al., *Long-term beneficial effect of protease inhibitors on the intrinsic apoptosis of peripheral blood mononuclear cells in HIV-infected patients.* HIV Med, 2012. **13**(8): p. 469-78.
22. Baca, L.M., et al., *Regulation of interferon-alpha-inducible cellular genes in human immunodeficiency virus-infected monocytes.* J Leukoc Biol, 1994. **55**(3): p. 299-309.
23. Krishnan, S., et al., *Evidence for innate immune system activation in HIV type 1-infected elite controllers.* J Infect Dis, 2014. **209**(6): p. 931-9.
24. Yu, X., et al., *Glycosphingolipid-functionalized nanoparticles recapitulate CD169-dependent HIV-1 uptake and trafficking in dendritic cells.* Nat Commun, 2014. **5**: p. 4136.
25. van der Kuyl, A.C., et al., *Sialoadhesin (CD169) expression in CD14+ cells is upregulated early after HIV-1 infection and increases during disease progression.* PLoS One, 2007. **2**(2): p. e257.
26. Clark, E., et al., *Loss of G(1)/S checkpoint in human immunodeficiency virus type 1-infected cells is associated with a lack of cyclin-dependent kinase inhibitor p21/Waf1.* J Virol, 2000. **74**(11): p. 5040-52.
27. Yi, L., et al., *Gene expression profiling of CD4(+) T cells in treatment-naive HIV, HCV mono- or co-infected Chinese.* Virol J, 2014. **11**: p. 27.

28. Benga, O. and V.J. Huber, *Brain water channel proteins in health and disease.* Mol Aspects Med, 2012. **33**(5-6): p. 562-78.
29. Johnson, T.P., et al., *Induction of IL-17 and nonclassical T-cell activation by HIV-Tat protein.* Proc Natl Acad Sci U S A, 2013. **110**(33): p. 13588-93.
30. Demacq, C., et al., *A genetic polymorphism of matrix metalloproteinase 9 (MMP-9) affects the changes in circulating MMP-9 levels induced by highly active antiretroviral therapy in HIV patients.* Pharmacogenomics J, 2009. **9**(4): p. 265-73.
31. Saha, R.N. and K. Pahan, *Differential regulation of Mn-superoxide dismutase in neurons and astroglia by HIV-1 gp120: Implications for HIV-associated dementia.* Free Radic Biol Med, 2007. **42**(12): p. 1866-78.
32. Manetti, F., *HIV-1 proteins join the family of LIM kinase partners. New roads open up for HIV-1 treatment.* Drug Discov Today, 2012. **17**(1-2): p. 81-8.
33. Wu, Y. and A. Yoder, *Chemokine coreceptor signaling in HIV-1 infection and pathogenesis.* PLoS Pathog, 2009. **5**(12): p. e1000520.
34. Solis, M., et al., *Gene expression profiling of the host response to HIV-1 B, C, or A/E infection in monocyte-derived dendritic cells.* Virology, 2006. **352**(1): p. 86-99.
35. Swingler, S., et al., *Apoptotic killing of HIV-1-infected macrophages is subverted by the viral envelope glycoprotein.* PLoS Pathog, 2007. **3**(9): p. 1281-90.
36. Milev, M.P., et al., *Characterization of staufen1 ribonucleoproteins by mass spectrometry and biochemical analyses reveal the presence of diverse host proteins associated with human immunodeficiency virus type 1.* Front Microbiol, 2012. **3**: p. 367.
37. Sarkar, R., D. Mitra, and S. Chakrabarti, *HIV-1 gp120 protein downregulates Nef induced IL-6 release in immature dentritic cells through interplay of DC-SIGN.* PLoS One, 2013. **8**(3): p. e59073.

Table S5. Quantitative real time PCR validations of differentially expressed ge
NOTE: The numbers are the ratios of gene expression levels (obtained by RKPM for
Red colour filled boxes show statistically significantly HAART up-regulated genes
significantly HAART down-regulated genes. Unfilled boxes indicate data without a
colour words show the names the HAART up-regulated genes in HIV patient; Yellow c
genes in HIV patient; Blue words show the DEGs shared by the HIV-TB patients (P1
in the healthy controls (H1 & H2).

Gene symbol	Method	the ratio of the RNA quantitative values after to before ART					Gene symbol	Method
		P1	P2	P3	H1	H2		
ACSL1	RNA-Seq	3.2635	2.4315	2.7229	0.9968	0.6288	CD160	RNA-Seq
	qRT-PCR	1.6029	33.6249	7.6038	0.0687	1.6479		qRT-PCR
GPR84	RNA-Seq	8.6796	19.3685	14.2573	0.9353	2.4498	CD244	RNA-Seq
	qRT-PCR	3.9818	8.2386	94.2039	0.0854	1.3284		qRT-PCR
ADM	RNA-Seq	3.1489	7.387	7.4553	1.6901	1.4275	IFIT1	RNA-Seq
	qRT-PCR	3.3162	10.5165	5.4921	0.6224	0.9454		qRT-PCR
S100P	RNA-Seq	6.4643	6.6343	7.8911	2.2672	0.9208	IFI44	RNA-Seq
	qRT-PCR	7.1842	13.7958	11.3421	2.4564	1.3212		qRT-PCR
AQP9	RNA-Seq	2.6995	3.6709	5.1539	1.1147	0.9644	IFI44L	RNA-Seq
	qRT-PCR	1.4275	6.3189	5.5087	0.3968	0.419		qRT-PCR
GPR97	RNA-Seq	5.1267	6.395	11.1236	0.7647	3.236	IFI27	RNA-Seq
	qRT-PCR	11.5316	9.0369	10.6605	0.1028	0.0781		qRT-PCR
BASP1	RNA-Seq	4.9045	2.713	4.9778	1.0105	1.6471	Mx1	RNA-Seq
	qRT-PCR	1.6054	2.3649	3.3525	0.0588	2.0155		qRT-PCR
MMP9	RNA-Seq	19.1131	19.4881	9.8669	0.6384	2.429	CX3CR1	RNA-Seq
	qRT-PCR	17.9598	1.3735	6.0613	0.7166	3.1033		qRT-PCR
SOD2	RNA-Seq	3.002	2.5947	4.7298	1.2455	0.6661	SIGLEC1	RNA-Seq
	qRT-PCR	1.663	2.4123	4.2212	0.6572	0.983		qRT-PCR
LRG1	RNA-Seq	12.5075	5.9117	4.5421	1.1487	0.504	PATL2	RNA-Seq
	qRT-PCR	2.2944	7.638	33.8234	0.1231	1.1661		qRT-PCR
LIMK2	RNA-Seq	4.9533	2.0229	2.9232	1.1339	1.0012	RASSF1	RNA-Seq
	qRT-PCR	3.7711	3.0229	3.5393	0.0423	2.237		qRT-PCR
IL1R2	RNA-Seq	16.8083	5.2271	10.2704	0.8588	0.2645	RNU2-1	RNA-Seq
	qRT-PCR	2.3841	3.0773	3.9276	0.0933	0.0172		qRT-PCR
BCL2A1	RNA-Seq	2.2714	2.1709	2.9246	1.7223	0.8152	SFXN1	RNA-Seq
	qRT-PCR	1.615	6.2051	3.3212	0.902	0.8447		qRT-PCR
CXCL1	RNA-Seq	2.3251	7.7073	10.2766	2.8546	0.4773	SOCS3	RNA-Seq
	qRT-PCR	1.5463	6.077	7.3214	1.0614	1.7898		qRT-PCR
							CDKN1C	RNA-Seq
								qRT-PCR

nes
RNA-Seq and qRT-PCR) of after/before HAART.
; and yellow colour filled boxes are
statistical significance (P>0.001). Red
colour words show the HAART down-regulated
and P2); Pink words show the DEG determined

the ratio of the RNA quantitative values after to before ART				
P1	**P2**	**P3**	**H1**	**H2**
0.3555	0.2572	0.1424	0.8154	0.6999
0.3301	0.1442	0.1141	0.0624	1.904
0.4647	0.3925	0.4051	0.869	0.6537
0.2836	0.3563	0.3663	0.2394	2.078
0.4261	0.1271	0.2563	0.8252	0.746
0.3609	0.3219	0.2384	0.4323	2.7942
0.3885	0.4709	0.3065	0.7473	0.7289
0.2839	0.0186	0.0217	0.111	2.0096
0.2591	0.1058	0.0878	0.6188	0.4146
0.2983	0.2966	0.1981	0.4313	0.992
0.1064	0.1005	0.0777	0.205	0.2854*
0.1655	0.0417	0.0573	0.0149	0.8586
0.4985	0.398	0.2485	0.9474	0.7496
0.3741	0.7309	0.2137	0.4185	1.2033
0.3974	0.4351	0.1999	0.9036	0.5644
0.1353	0.5893	0.5787	0.2619	0.242
0.0531	0.0181	0.0359	1.3492	0.4373
0.0298	0.2325	0.032	0.7072	2.1963
0.4721	0.2537	0.3161	0.8557	0.5803
0.5176	0.8149	0.3946	0.128	1.5548
0.4727	0.4765	0.4918	0.6594	1.2838
0.0909	0.8922	0.3156	0.0174	1.3913
0.523	2.487	1.0465	0.1002	0.4571
0.5162	4.421	1.9501	0.0821	0.2086
2.0863	2.1977	1.4087	1.1267	1.6689
1.7206	6.0214	4.1821	0.2179	2.8734
2.4823	2.4005	1.8402	1.1382	0.7431
1.9737	2.9656	2.8918	0.4732	2.0134
0.1088	0.1365	0.2654*	0.8082	0.6689
0.1058	0.2964	0.6368	0.063	0.0035

GO	Class	No. up-regu
biological_	biological a	0
biological_	biological r	13
biological_	cell prolifer	3
biological_	cellular cor	4
biological_	cellular pro	14
biological_	death	5
biological_	developme	6
biological_	establishm	2
biological_	growth	1
biological_	immune sy	6
biological_	localizatior	4
biological_	locomotior	3
biological_	metabolic p	6
biological_	multi-orgar	2
biological_	multicellula	9
biological_	negative re	5
biological_	pigmentati	1
biological_	positive reg	4
biological_	regulation	11
biological_	reproductic	2
biological_	reproductiv	2
biological_	response to	10
biological_	signaling	6
cellular_co	cell	12
cellular_co	cell part	12
cellular_co	extracellula	3
cellular_co	extracellula	3
cellular_co	macromole	1
cellular_co	membrane	1
cellular_co	organelle	6
cellular_co	organelle p	4
molecular_	antioxidant	1
molecular_	binding	9
molecular_	catalytic ac	4
molecular_	enzyme reg	2
molecular_	molecular t	1
molecular_	receptor ac	1
molecular_	transporter	1

Up-regulated genes
-
AQP9;ADM;SOD2;GPR97;LIMK2;SOCS3;MMP9;S100P;SFXN1;CXCL1;BCL2A1;ACSL1;GPR84
ADM;CXCL1;SOD2
SOD2;MMP9;ADM;CXCL1
ADM;SOD2;GPR97;LIMK2;SOCS3;MMP9;S100P;AQP9;CXCL1;SFXN1;BCL2A1;ACSL1;GPR84;LRG1
SOD2;BCL2A1;SOCS3;MMP9;ADM
SOD2;ADM;SOCS3;MMP9;SFXN1;LRG1
SFXN1;AQP9
SOCS3
MMP9;SFXN1;SOD2;AQP9;CXCL1;IL1R2
SFXN1;MMP9;AQP9;S100P
MMP9;CXCL1;S100P
ADM;SOD2;LIMK2;SOCS3;ACSL1;MMP9
ADM;SOCS3
ADM;LIMK2;AQP9;S100P;MMP9;SOD2;SFXN1;SOCS3;ACSL1
ADM;CXCL1;SOD2;BCL2A1;SOCS3
SOD2
ADM;SOD2;MMP9;SOCS3
ADM;GPR97;SOD2;LIMK2;SOCS3;MMP9;S100P;CXCL1;BCL2A1;ACSL1;GPR84
LIMK2;ADM
LIMK2;ADM
AQP9;ADM;SOD2;GPR97;SOCS3;CXCL1;ACSL1;GPR84;S100P;IL1R2
GPR97;S100P;SOCS3;GPR84;ADM;CXCL1
BASP1;ACSL1;SFXN1;SOD2;LIMK2;AQP9;LRG1;GPR84;GPR97;ADM;S100P;IL1R2
BASP1;ACSL1;SFXN1;SOD2;LIMK2;AQP9;LRG1;GPR84;GPR97;ADM;S100P;IL1R2
ADM;CXCL1;MMP9
ADM;CXCL1;MMP9
AQP9
SOD2
BASP1;ACSL1;SFXN1;SOD2;LIMK2;LRG1
ACSL1;SFXN1;SOD2;LIMK2
SOD2
MMP9;SOD2;LIMK2;ACSL1;SFXN1;CXCL1;S100P;IL1R2;ADM
SOD2;MMP9;LIMK2;ACSL1
CXCL1;SOCS3
IL1R2
IL1R2
AQP9

No. down-r	Down-regulated genes
2	SIGLEC1;CX3CR1
6	CDKN1C;RASSF1;MX1;PATL2;CD160;CX3CR1
1	CDKN1C
1	PATL2
7	CDKN1C;RASSF1;MX1;SIGLEC1;PATL2;CD160;CX3CR1
1	MX1
1	CDKN1C
0	-
0	-
1	IFI44L
0	-
1	CX3CR1
2	CDKN1C;PATL2
2	IFI44;MX1
1	CDKN1C
3	CDKN1C;RASSF1;PATL2
0	-
2	MX1;CDKN1C
6	CDKN1C;RASSF1;MX1;PATL2;CD160;CX3CR1
0	-
0	-
8	CDKN1C;RASSF1;CX3CR1;SIGLEC1;IFI44;MX1;CD160;IFI44L
4	CDKN1C;RASSF1;CD160;CX3CR1
9	PATL2;RASSF1;CD160;CD244;CX3CR1;SIGLEC1;CDKN1C;IFI27;MX1
9	PATL2;RASSF1;CD160;CD244;CX3CR1;SIGLEC1;CDKN1C;IFI27;MX1
0	-
0	-
2	PATL2;RASSF1
1	CDKN1C
3	RASSF1;CDKN1C;PATL2
2	CDKN1C;RASSF1
0	-
5	CX3CR1;MX1;PATL2;RASSF1;SIGLEC1
1	MX1
1	CDKN1C
2	CX3CR1;CD160
2	CX3CR1;CD160
0	-

gene_name	gene_id	log2Ratio(P1-3W0/H1-2W0)	probability
GBP2	2634	1.16538582	0.810102174
REC8	9985	1.78562432	0.803503456
SERPING1	710	4.03737325	0.913527998
RSAD2	91543	3.957803761	0.911812581
CD8B	926	1.492125445	0.847941501
CD38	952	1.763209738	0.836697386
ISG15	9636	2.964163193	0.914629871
DUSP2	1844	1.20185218	0.818879595
TRIM22	10346	1.352712235	0.833542021
DEFA4	1669	4.548287623	0.915969648
EGR2	1959	2.076514159	0.869465592
UBE2L6	9246	1.171467765	0.809601322
USP18	11274	3.617106812	0.889624862
CXCR2P1	3580	1.641330363	0.823086747
STAT1	6772	2.018311458	0.883101272
IGJ	3512	1.772408374	0.874273765
BPGM	669	1.537705167	0.827631974
SAMD9L	219285	1.480216584	0.818754382
OAS1	4938	1.510729019	0.841543123
CCL2	6347	2.470056103	0.87051738
HELZ2	85441	1.561662116	0.802326455
HERC5	51191	2.251125148	0.852837323
IFIT1B	439996	5.344627464	0.833892617
DEFA3	1668	4.885945931	0.954973455
AHSP	51327	5.234315115	0.9522939
RAP1GAP	5909	7.094227082	0.832590404
HLA-DRB4	3126	9.629255004	0.984673946
RGS1	5996	1.262964965	0.806683863
SIGLEC1	6614	4.76034878	0.927401583
GBP5	115362	2.032806139	0.881661324
CD8A	925	1.787166248	0.871331263
HBD	3045	5.634450818	0.968534008
IFI44	10561	2.997462039	0.908306621
CLC	1178	1.693672242	0.845938095
ELANE	1991	3.741351203	0.848955725
IRF7	3665	1.703887217	0.857006912
EPSTI1	94240	2.725875583	0.90274717
HBG2	3048	1.974864012	0.866660823
IGLL5	100423062	1.187871736	0.818791946
SELENBP1	8991	4.761776345	0.924734549
MIR5047	100616408	1.98938992	0.804430031
MYL4	4635	2.724007171	0.801387359
LAG3	3902	1.720486167	0.828508464
OAS2	4939	1.937650696	0.874248723
CTSG	1511	3.954614514	0.813295102
DDX60	55601	1.917395194	0.830937594
CA1	759	4.213682382	0.922630973
GBP1	2633	2.962299857	0.903298107
EGR1	1958	1.256771365	0.82486477

LENG8	114823	1.366086453	0.822085045
PHOSPHO1	162466	2.151918066	0.825878994
HBG1	3047	3.750688686	0.909571271
MZB1	51237	1.577874427	0.837874386
CTLA4	1493	1.72275305	0.804868276
APOL6	80830	1.585000512	0.838162376
SLC25A39	51629	1.913617742	0.877316438
OR2W3	343171	3.255069797	0.81668837
MX1	4599	2.583429422	0.898114294
PARP9	83666	2.01914789	0.858784934
CMPK2	129607	3.000742425	0.893130822
SLC4A1	6521	4.599493665	0.929492637
ATHL1	80162	1.526619683	0.827268857
IFI44L	10964	4.743047682	0.944192627
LGALS3BP	3959	2.745738341	0.896686868
PARP12	64761	1.438693229	0.807648002
IFITM1	8519	1.186697694	0.820857959
STRADB	55437	1.978767099	0.858046179
NEAT1	283131	1.238917156	0.812869378
ETV7	51513	3.675599822	0.828771411
IFI35	3430	1.560183048	0.843283582
WARS	7453	1.125513152	0.805869979
HBB	3043	3.229330213	0.923344686
TNFSF10	8743	1.285005213	0.819643394
CCR5	1234	2.078804897	0.82739407
LAP3	51056	1.435650463	0.83985275
OTOF	9381	5.72665435	0.911098868
IFI27	3429	8.433015745	0.995079135
IRF9	10379	1.277148206	0.813758389
IFIT3	3437	4.197284404	0.933687268
TAP1	6890	1.132485754	0.80374136
HBA2	3040	4.172356065	0.943215967
OASL	8638	2.560564967	0.882412601
PATL2	197135	2.04742109	0.861765001
HES4	57801	3.421591964	0.810177301
ALAS2	212	4.929701312	0.956363318
OAS3	4940	2.605393463	0.894633377
KLHDC7B	113730	2.630618651	0.863593108
TRIM58	25893	1.802496925	0.815160773
EPB42	2038	4.945885516	0.876552639
MCOLN2	255231	2.435740185	0.801963338
BCL2L1	598	1.921406559	0.871656817
LY6E	4061	2.051243055	0.890150756
IFI6	2537	2.937837611	0.91404137
NPDC1	56654	2.301245166	0.812143143
PCSK1N	27344	4.396454608	0.890776821
LCN2	3934	2.967786287	0.888347691
GMPR	2766	2.397798552	0.851622759
ELK2AP	2003	1.583784524	0.85008264
MT1X	4501	1.177704491	0.807610438

CXCL10	3627	3.800602584	0.876540118
MIAT	440823	1.67335837	0.827444155
GBP4	115361	1.558990041	0.829222178
LTF	4057	3.920873159	0.909120505
CAMP	820	3.710881598	0.877779726
MT1E	4493	2.01353491	0.872620956
TKTL1	8277	2.766594165	0.868989783
SNCA	6622	2.79189947	0.892141641
MT2A	4502	1.433649226	0.845512371
TNFRSF17	608	2.102477288	0.813019633
RETN	56729	1.288951528	0.804505159
HBA1	3039	4.501465194	0.951567665
IFIT1	3434	4.197311662	0.928328158
DMTN	2039	1.671493185	0.842845337
DEFA1	1667	4.843900077	0.844160072
EIF2AK2	5610	1.812503548	0.83031153
AZU1	566	2.885392092	0.801475008
SLC25A37	51312	1.866656666	0.863931183
PARP14	54625	1.669917383	0.842306922
IFITM3	10410	2.238678529	0.897863869
HBM	3042	5.396215519	0.950478313
FBXO7	25793	1.124142881	0.800585996
TYMS	7298	2.473358412	0.813332666
MX2	4600	1.871766463	0.866122408
IFIT2	3433	2.904769873	0.897400581
XAF1	54739	1.817719469	0.86711159
RPS26	6231	2.508430124	0.905326555
ODF3B	440836	1.488694211	0.828621156
FCGR3B	2215	2.048695483	0.875438245
LYSMD1	388695	3.372828356	0.814672443

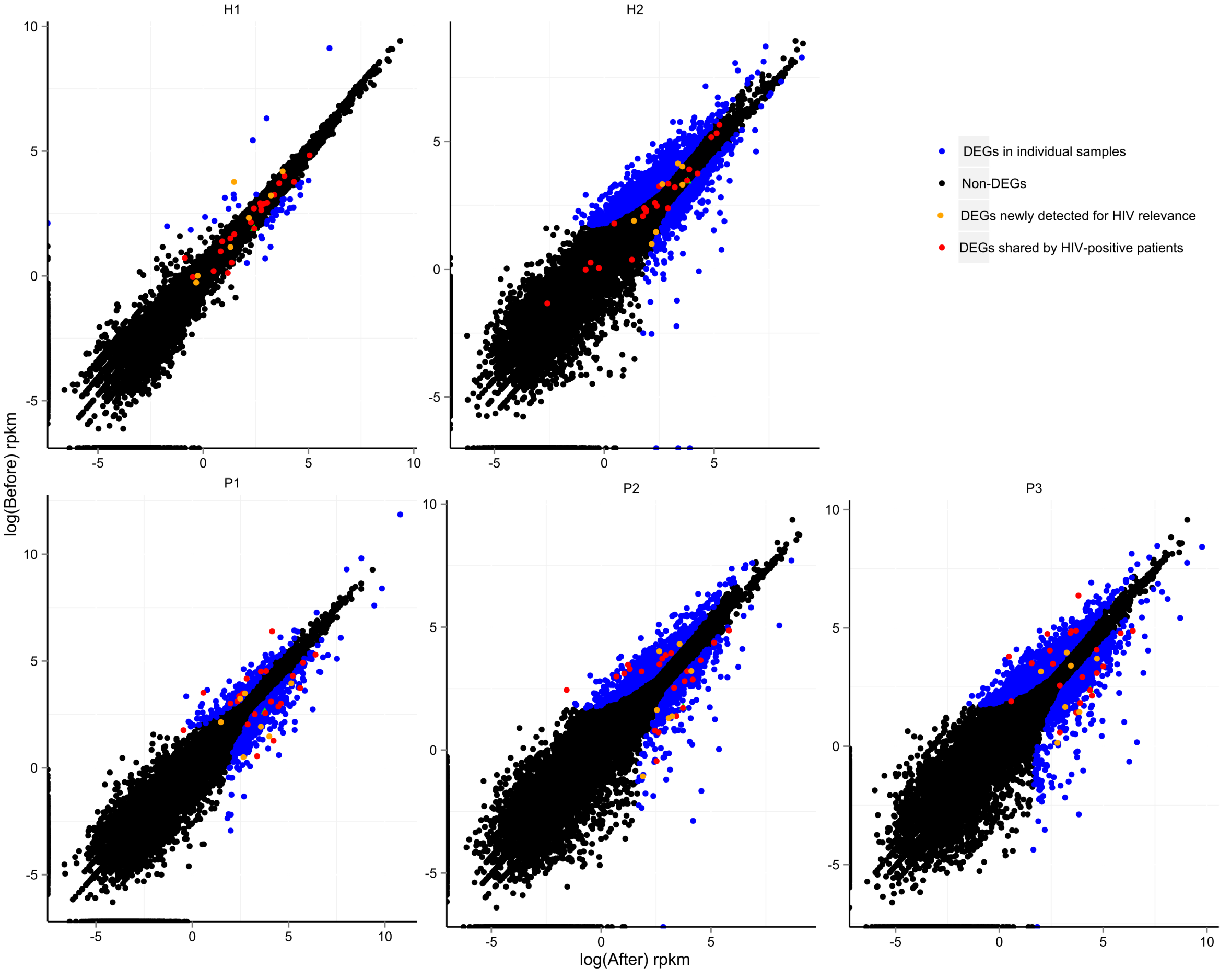
H1
H2
P1
P2
P3
log(Before) rpkm
log(After) rpkm
DEGs in individual samples
Non-DEGs
DEGs newly detected for HIV relevance
DEGs shared by HIV-positive patients

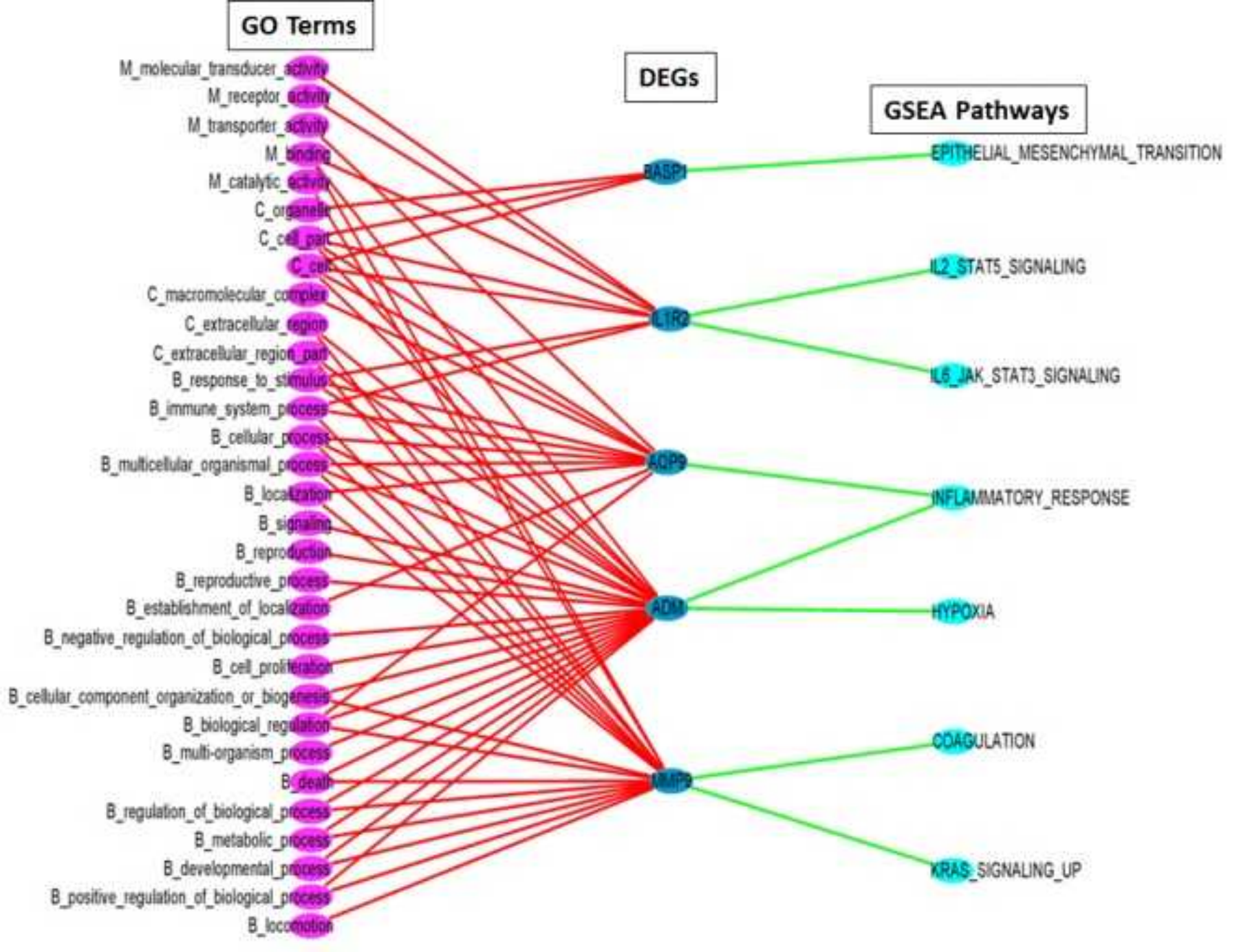
GO Terms
DEGs
GSEA Pathways
M_molecular_transducer_activity
M_receptor_activity
M_transporter_activity
M_binding
M_catalytic_activity
C_organelle
C_cell_part
C_cell
C_macromolecular_complex
C_extracellular_region
C_extracellular_region_part
B_response_to_stimulus
B_immune_system_process
B_cellular_process
B_multicellular_organismal_process
B_localization
B_signaling
B_reproduction
B_reproductive_process
B_establishment_of_localization
B_negative_regulation_of_biological_process
B_cell_proliferation
B_cellular_component_organization_or_biogenesis
B_biological_regulation
B_multi-organism_process
B_death
B_regulation_of_biological_process
B_metabolic_process
B_developmental_process
B_positive_regulation_of_biological_process
B_locomotion
BASP1
IL1R2
ADM
MMP9
EPITHELIAL_MESENCHYMAL_TRANSITION
IL2_STAT5_SIGNALING
IL6_JAK_STAT3_SIGNALING
INFLAMMATORY_RESPONSE
HYPOXIA
COAGULATION
KRAS_SIGNALING_UP